

Créteil, July 19, 2017

Object: Revised version, manuscript COMMAT-D-17-00680

Dear Professor Jeffrey Hoyt,

Thank you for the opportunity you gave us to revise our Manuscript COMMAT-D-17-00680 entitled “From morphology to thermodynamics and mechanical properties of epoxy/clay nanocomposite: investigation by molecular dynamics simulations” by Van Son Vo, Vu-Hieu Nguyen, Samia Mahouche-Chergui, Benjamin Carbonnier, Devis Di Tommaso and Salah Naili.

As suggested by the referee 3, the title of the revised manuscript is henceforth “From atomistic structure to thermodynamics and mechanical properties of epoxy/clay nanocomposites: investigation by molecular dynamics simulations”.

You will find with this letter for your convenience a point-by-point answer to the points made by the referees. All of the changes are explained in detail. We deal with the points sequentially, with their comments indented in a small font size and our response in a normal font size.

Given the overall positive recommendations of the referees, we trust that the manuscript is now acceptable for publication in Computational Materials Science.

Correspondence should be addressed to Professor S. Naili.

With all best wishes,

Salah NAILI,
on behalf of the authors.

Créteil, July 18, 2017

Response to the referee on the Manuscript COMMAT-D-17-00680 presented by Van Son Vo *et al.*

via

Professor Jeffrey Hoyt (Editor)
Computational Materials Science

Dear referee,

Thank you for the opportunity you gave us to revise our Manuscript COMMAT-D-17-00680 entitled “From morphology to thermodynamics and mechanical properties of epoxy/clay nanocomposite : investigation by molecular dynamics simulations” by Van Son Vo, Vu-Hieu Nguyen, Samia Mahouche-Chergui, Benjamin Carbonnier, Devis Di Tommaso and Salah Naili.

We thank the referee for his helpful and comments regarding our work and we are pleased that his opinion is “It establishes a clear computational methodology to simulate the properties of PCNs. So, I will recommend this draft to publish on the journal of Computational Materials Science.”.

As suggested by one of the referees, the title of the revised manuscript is henceforth “From atomistic structure to thermodynamics and mechanical properties of epoxy/clay nanocomposites : investigation by molecular dynamics simulations”.

Please see our detailed responses below. As a result of the comments, we have modified the paper and we hope that the referee will be satisfied with the revised version.

Referee comment :

“This work presents a novel method to study the structural and mechanical properties of complicated polymer/clay nanocomposites, combining several different levels of computational approaches and analyses. This draft provides atomic insights to study PCNs and is able to compute the related thermodynamic and elastic properties of the

multi-functional materials. It establishes a clear computational methodology to simulate the properties of PCNs. So, I will recommend this draft to publish on the journal of Computational Materials Science.”

Author response :

We thank the referee for his positive evaluation of our manuscript and for his support for the publication of our manuscript in Computational Materials Science.

Referee comment :

“In general, the figures are nice. However, if fussily, nearly all the fonts of the labels of x- and y-axis as well as the legends are smaller than their captions and text. It would be great if those labels can be enlarged. Particularly Figure 3, the atoms are too small to be clearly viewed. I will suggest the authors enlarging the four snaps of Figure 3, also the atomic labels.”

Author response :

The font size of the labels and of the legends has been increased to improve the readability the Figure’s text.

Salah NAILI,
on behalf of the authors.

Créteil, July 18, 2017

Response to the referee on the Manuscript COMMAT-D-17-00680 presented by Van Son Vo *et al.*

via

Professor Jeffrey Hoyt (Editor)
Computational Materials Science

Dear referee,

Thank you for the opportunity you gave us to revise our Manuscript COMMAT-D-17-00680 entitled “From morphology to thermodynamics and mechanical properties of epoxy/clay nanocomposite : investigation by molecular dynamics simulations” by Van Son Vo, Vu-Hieu Nguyen, Samia Mahouche-Chergui, Benjamin Carbonnier, Devis Di Tommaso and Salah Naili.

We thank the referee for his helpful and comments regarding our work and we are pleased that his opinion is “The calculations have been carried out with care and are reproducible. The results on mechanical properties are interesting, and the reported elastic constants and radial distribution functions contribute to better understanding of composite properties.”

As suggested by one of the referees, the title of the revised manuscript is henceforth “From atomistic structure to thermodynamics and mechanical properties of epoxy/clay nanocomposites : investigation by molecular dynamics simulations”.

Please see our detailed responses below. As a result of the comments, we have modified the paper and we hope that the referee will be satisfied with the revised version.

Referee comment :

“The authors report a study of mechanical properties of a model clay/epoxy polymer composite. I am somewhat confused about the model choices. The clay parameters in CLAYFF are not suited to study interfacial adsorption and binding mechanisms - they are good for high temperature glasses only. Some sources have shown that

cleavage and organic binding energies are 100% off compared to experiment whereas interface FF gives ; 10% deviation. See, for example, Chem. Mater. 2005, 17, 5658, and a review in Clay Miner. 2012, 47, 205. The reason for this are poor choices of atomic charges in CLAYFF that do not reproduce dipole moments and interfacial interactions. I think the authors should discuss these issues and references in the paper as the assumptions affect the reported results. It is known that CLAYFF can calculate better mechanical properties than Interface FF as many bonding terms therein plus the nonbond terms overestimate the in-plane stiffness (J. Phys. Chem. C 2010, 114, 1763). These differences, however, have little impact at low filler fraction.”

Author response :

We agree with referee that InterfaceFF would give more accurate cleavage energies and binding energies for the PCNs system. However, these quantities have not been computed in the present work because its main goal was to evaluate the thermodynamic and mechanical properties of PCNs at different temperatures temperature (300 K to 600 K). Moreover, InterfaceFF contains several intramolecular terms that can overestimate the in-plane stiffness of the PCNs system [1] and increase the computation time of the molecular dynamics simulations. Given that the CLAYFF force field has been previously adopted to calculate the structural and mechanical properties of clays and other PCNs systems [1, 2, 3, 4], given that CLAYFF has a rather simple functional form, which makes this force field computationally fast and robust for the simulation of multicomponent systems, CLAYFF is a suitable potential model to accurately simulate the structural and thermodynamic properties of epoxy/clay nanocomposite.

The following paragraph and references given below have been added to the revised manuscript at the end of Section 2.3 ”Force field description”.

Given that the CLAYFF forcefield has been previously adopted to calculate the structural and mechanical properties of clays and other PCNs systems [2, 3, 4, 5, 6], given that CLAYFF has a rather simple functional form, which makes this forcefield computationally fast and robust for the simulation of multicomponent complex systems, CLAYFF is a suitable potential model to accurately simulate the structural and thermodynamic properties of epoxy/clay nanocomposite. It was previously pointed out that this forcefield is not appropriate to compute cleavage and binding energies [1, 7, 8], but the evaluation of these properties is not the focus of the present study.

[1] Heinz, H. (2012). Clay minerals for nanocomposites and biotechnology : surface modification, dynamics and responses to stimuli. Clay Minerals, 47(2), 205-230.

[2] Mazo, M.A., Manevitch, L.I., Gusarova, E.B., Shamaev, M.Y., Berlin, A.A., Balabaev, N.K., Rutledge, G.C. (2008). Molecular dynamics simulation of thermomechanical properties of montmorillonite crystal. 1. Isolated clay nanoplate. The Journal of Physical Chemistry B, 112(10), 2964-2969.

[3] Liu, X., Lu, X., Wang, R., Zhou, H., Xu, S. (2007). Interlayer structure and dynamics of alkylammonium-intercalated smectites with and without water : A molecular dynamics study. Clays and Clay Minerals, 55(6), 554-564.

[4] Anoukou, K., Zaoui A., Zaïri F., Nait-Abdelaziz, M., Gloaguen, J.-M. (2013). Molecular dynamics study of the polymer clay nanocomposites (PCNs) : Elastic constants and basal spacing predictions, *Computational Materials Science*, 77, 417-423.

[5] Suter, J.L., Coveney, P.V. (2009). Computer simulation study of the materials properties of intercalated and exfoliated poly (ethylene) glycol clay nanocomposites. *Soft Matter*, 5(11), 2239-2251.

[6] Carrier, B., Vandamme, M., Pellenq, R.J.M., Van Damme, H. (2014). Elastic properties of swelling clay particles at finite temperature upon hydration. *The Journal of Physical Chemistry C*, 118(17), 8933-8943.

[7] Heinz, H., Koerner, H., Anderson, K.L., Vaia, R.A., Farmer, B.L. (2005). Force field for mica-type silicates and dynamics of octadecylammonium chains grafted to montmorillonite. *Chemistry of materials*, 17(23), 5658-5669.

[8] Zartman, G.D., Liu, H., Akdim, B., Pachter, R., Heinz, H. (2010). Nanoscale tensile, shear, and failure properties of layered silicates as a function of cation density and stress. *The Journal of Physical Chemistry C*, 114(4), 1763-1772.

The following criteria have been used to verify the accuracy of the molecular model and simulations :

- The structural parameters obtained from the density profile of the epoxy matrix as well as the polymer confined between the clay layers agree with experimental characterisation of PCNs reported in the literature [9, 10, 11].
- The presence of the interphase revealed in our study was inferred by Chen et al. [12].
- The elastic tensors obtained from our simulations for the PCNs system are agree with the orthorhombic symmetry [13].
- The CLAYFF forcefield has been widely previously adopted to calculate the structural and mechanical properties of clays.

The following paragraph has been added to the revised manuscript in section 2.1.

It is also important to point out that the molecular models used in this manuscript are "clay clusters" and not true PCNs. Real PCNs should be the mixture of clay clusters with polymer matrix, and they have a very complex structure [12, 13]. Therefore, a comparison with the real PCNs in the experimental part will be not appropriate. Moreover, it should be noted that, in the experimental part, it is impossible to make the nanocomposites with a specific control interlayer distance. Thus, the molecular dynamics simulation has been used to investigate the properties of the nanocomposites.

[9] Tack, J L., Ford, D.M. (2008). Thermodynamic and mechanical properties of epoxy resin DGEBF crosslinked with DETDA by molecular dynamics. *Journal of Molecular Graphics and Modelling*, 26(8), 1269-1275.

[10] Fan, H.B., Yuen, M.M. (2007). Material properties of the cross-linked epoxy resin compound predicted by molecular dynamics simulation. *Polymer*, 48(7), 2174-2178.

[11] Chen, Y., Chia, J.Y.H., Su, Z.C., Tay, T.E., Tan, V.B.C. (2013). Mechanical characterization of interfaces in epoxy-clay nanocomposites by molecular simulations. *Polymer*, 54(2), 766-773.

[12] Suter, J.L., Coveney, P.V. (2009). Computer simulation study of the materials properties of intercalated and exfoliated poly (ethylene) glycol clay nanocomposites. *Soft Matter*,

5(11), 2239-2251.

[13] Anoukou, K., Zaoui A., Zaïri F., Nait-Abdelaziz, M., Gloaguen, J.-M. (2013). Molecular dynamics study of the polymer clay nanocomposites (PCNs) : Elastic constants and basal spacing predictions,” Computational Materials Science, 77, 417-423.

Referee comment :

“Can the authors confirm the (supposedly) correct in-plane modulus of neat montmorillonite of 160 GPa (+/-10 GPa) in their calculations?”

Author response :

In the literature, the values of the in-plane *moduli* E_{xx} and E_{yy} of neat montmorillonite layer are in the range of 160 – 400 GPa (see Tab. 1).

Authors	h (nm)	E_{xx} (GPa)	E_{yy} (GPa)
Manevitch <i>et al.</i> [15]	1-0.6	250-420	250-420
Mazo <i>et al.</i> [16]	0.6-0.65	442	399
Suter <i>et al.</i> [17]	6.69-9.37	210-331	245-356
Carrier <i>et al.</i> [18]	0.656	292.3	274.2
Xu <i>et al.</i> [19]	0.615	277	277.8
Zartman <i>et al.</i> [20]	0.955	160	160

TABLE 1 – Values of the in-plane *moduli* E_{xx} and E_{yy} of neat montmorillonite layer issues of the literature.

It should be noted that the thickness of clay layer is small (around to 0.65 nm), this is why the molecular model with only clay layer can not be computed because the limit of R_{cut} . Basically, in order to overcome this problem, the calculation was performed with the interlayer distance in the literature. The reported value in Tab. 1 was determined in function of the thickness of the clay layer. Moreover, the method using stress-strain behavior seems to be more suitable to determine the mechanical properties of clay layer. In this study, we used the strain fluctuations method for determining the mechanical properties of the PCNs system. Due to the issues mentioned above, we are not able to confirm the value of the in-plane *modulus* of neat montmorillonite of 160 GPa (± 10 GPa). However, the value of 160 – 230 GPa used for the in-plane *modulus* of neat montmorillonite layer in the calculation with the finite element method give results suitable.

[15] Manevitch, O.L., Rutledge, G.C. (2004). Elastic properties of a single lamella of montmorillonite by molecular dynamics simulation. The Journal of Physical Chemistry B, 108(4), 1428-1435.

[16] Mazo, M.A., Manevitch, L.I., Gusarova, E.B., Shamaev, M.Y., Berlin, A.A., Balabaev, N.K., Rutledge, G.C. (2008). Molecular dynamics simulation of thermomechanical

properties of montmorillonite crystal. 1. Isolated clay nanoplate. The Journal of Physical Chemistry B, 112(10), 2964-2969.

[17] Suter, J.L., Coveney, P.V., Greenwell, H.C., Thyveetil, M.A. (2007). Large-scale molecular dynamics study of montmorillonite clay : emergence of undulatory fluctuations and determination of material properties. The Journal of Physical Chemistry C, 111(23), 8248-8259.

[18] Carrier, B., Vandamme, M., Pellenq, R.J.M., Van Damme, H. (2014). Elastic properties of swelling clay particles at finite temperature upon hydration. The Journal of Physical Chemistry C, 118(17), 8933-8943.

[19] Xu, W., Zeng, Q., Yu, A. (2012). Young's modulus of effective clay clusters in polymer nanocomposites. Polymer, 53(17), 3735-3740.

[20] Zartman, G.D., Liu, H., Akdim, B., Pachter, R., Heinz, H. (2010). Nanoscale tensile, shear, and failure properties of layered silicates as a function of cation density and stress. The Journal of Physical Chemistry C, 114(4), 1763-1772.

Referee comment :

“The calculations have been carried out with care and are reproducible. The results on mechanical properties are interesting, and the reported elastic constants and radial distribution functions contribute to better understanding of composite properties.”

Author response :

We thank referee for the overall positive assessment and we anticipate that the new version of the manuscript is now acceptable for publication in Computational Materials Science.

Salah NAILI,
on behalf of the authors.

Créteil, July 19, 2017

Response to the referee on the Manuscript COMMAT-D-17-00680 presented by Van Son Vo *et al.*

via

Professor Jeffrey Hoyt (Editor)
Computational Materials Science

Dear referee,

Thank you for the opportunity you gave us to revise our Manuscript COMMAT-D-17-00680 entitled “From morphology to thermodynamics and mechanical properties of epoxy/clay nanocomposite : investigation by molecular dynamics simulations” by Van Son Vo, Vu-Hieu Nguyen, Samia Mahouche-Chergui, Benjamin Carbonnier, Devis Di Tommaso and Salah Naili.

We thank the referee for his helpful and comments regarding our work and we are pleased that his opinion is “This subject may be attractive.”.

Please see our detailed responses below. As a result of the comments, we have modified the paper and we hope that the referee will be satisfied with the revised version.

Referee comment :

“0. Authors claimed that they have proposed a novel molecular approach to study the morphology and thermomechanical properties of epoxy/clay nanocomposites. They utilized molecular dynamic simulations to determine structural arrangement of the constitutive components PCNs, the molecular interactions and the influence of silicate layer on the thermodynamic and elastic properties of these materials. Also, they investigated the thermodynamic properties of the confined polymer in each structure to characterize the role of silicate layer on the properties of nanocomposites. This subject may be attractive. However, the biggest challenge is its novelty, because the similar

works may be found in the literature. Therefore, I think that the authors should explain clearly the originality and novelty of their work as well as revise the manuscript substantially for consideration again.”

Author response :

Polymer/clay nanocomposites (PCNs) materials have been previously studied by means of computational methods but only few studies have considered the structure and thermodynamic properties of thermosetting polymers/clay nanocomposites (see reference 16 in the manuscript). To the best of our knowledge, this work reports the first computational model and molecular dynamics simulations of PCNs composed of silanized-clay and thermosetting epoxy resin. Three nanocomposite structures consisting of different representative cross-linked epoxy molecules were considered to represent intercalated or exfoliated structures.

To put this work in the context of previously published theoretical studies of PCN materials and to highlight our novel contribution to this field, the following text has been added in the section 1 ”Introduction”.

The molecular structures of intercalated and exfoliated poly ϵ -caprolactone (PCL) nanocomposites have been previously studied by means of the molecular dynamics (MD) technique [7, 8]. Gardebien et al. [7] investigated the effect of the number and length of polymer chains on the structure of intercalated nanocomposites. By examining the interlayer density profiles, the authors found that the interlayer phase organizes into four layers while the charged heads of the surfactants remained at the surface. On the other hand, for the exfoliated nanocomposites it was found a layered structure with high density of organic phase near the clay surface. The different arrangement of poly (ethylene oxide) (PEO) in the intercalated and exfoliated nanocomposites was considered by Suter and Coveney [9] using large-scale MD simulations, where non-modified montmorillonite (MMT-Na) was used to model the inorganic phase. It was found that the PEO chains organize in layers parallel to the clay surface, and because of the sodium ions and the charges within the clay surface the conformation of the polymer in the exfoliated structure was significantly different from the intercalated system.

Elastic coefficients of PCNs are important properties that can be used as parameters in continuum mechanical models to estimate other macroscopic properties of PCNs [10,11]. However, only Xu et al. has used computational methods to predict the longitudinal and lateral Young’s *moduli* of the exfoliated and partially intercalated/exfoliated clay clusters.

So far, computational models of PCNs were restricted to the cases of clay with pristine surface or chemically modified through cationic exchange with surfactant molecules.

In the works cited above, the pristine clay of organically modified clays with cationic surfactants were modelled. Modification of the clay surface by the covalent grafting was, for the first time, modelled using in the work of Piscitelli et al. [13]. Their MD simulations

revealed that an increase of aminosilanes concentration and the use of shorted aminosilane chains contribute to the extent of the d -spacing in the clay.

To the best of our knowledge, there is no computational study where these silanized clays served as fillers in polymer matrix, despite these techniques are extensively used in the synthesis of epoxy/clay nanocomposites [14, 15, 16, 17, 18]. Moreover, there is only a single computational study on the structural and thermosetting properties of polymer/clay nanocomposites [14], where Chen and co-workers considered intercalated and exfoliated clay-nanocomposites based on epoxy matrix cross-linked from Diglycidyl ether of bisphenol-A and Diethylmethylbenzenediamine (DGEBA and DETDA). In this study, a series of surfactants with a single ammonium group and one alkyl chain of various length were used and the failure behaviour of the interphase in terms of quantifiable parameters such as peak strength, fracture energy and final separation distance were determined. However, details of the molecular structures and overall thermomechanical properties of these nanocomposites were not investigated.

In the present work, we propose a molecular model based on the epoxy-based nanocomposite and silanized-clay models of Piscitelli et al. [13] to investigate the structural, thermodynamic and mechanical properties of thermosetting clay nanocomposites. The arrangements of the constitutive components of PCNs, and the effect of silicate layer on the thermodynamic and elastic properties of these multifunctional materials are quantified by means of molecular dynamics simulations of three nanocomposite structures consisting of different representative cross-linked epoxy molecules to represent intercalated or exfoliated structures.

Referee comment :

“1. Title does not represent the main work of the research? Please, revise it. ”

Author response :

In our manuscript, we introduced an atomistic model to study the structural, thermodynamic and mechanical properties of epoxy/clay nanocomposite using molecular dynamics simulations. It is the reason for which we slightly change the title to ”From atomistic structure to thermodynamics and mechanical properties of epoxy/clay nanocomposites : investigation by molecular dynamics simulations”.

Referee comment :

“2. Literature reviews are not complete. Many researches have been conducted on the issues raised in the manuscript. I recommend to add the manuscript the suitable references ; such as, (Molecular dynamics study of epoxy/clay nanocomposites : rheology and molecular confinement, Journal of Polymer Research 19 (6), 9897 , 2012), etc.”

Author response :

Previously published computational studies of PCNs are now referenced in the section 1 "Introduction".

Referee comment :

"3. Please, the necessity of performing this work should be clarified?"

Author response :

This point has been addressed in the response of the item 0.

Referee comment :

"4. What are the criteria for evaluating the accuracy of the obtained results? Also, is there any experimental data to check and compare the results?"

Author response :

The following criteria have been used to verify the accuracy of the molecular model and simulations :

- The structural parameters obtained from the density profile of the epoxy matrix as well as the polymer confined between the clay layers agree with experimental characterisation of PCNs reported in the literature [1, 2, 3].
- The presence of the interphase revealed in our study was inferred by Chen et al. [4].
- The elastic tensors obtained from our simulations for the PCNs system are agree with the orthorhombic symmetry [5].
- The CLAYFF force field has been widely previously adopted to calculate the structural and mechanical properties of clays.

The following paragraph has been added to the revised manuscript in section 2.1.

It is also important to point out that the molecular models used in this manuscript are "clay clusters" and not true PCNs. Real PCNs should be the mixture of clay clusters with polymer matrix, and they have a very complex structure [4, 5]. Therefore, a comparison with the real PCNs in the experimental part will be not appropriate. Moreover, it should be noted that, in the experimental part, it is impossible to make the nanocomposites with a specific controlled interlayer distance. Thus, the molecular dynamics simulation has been used to investigate the properties of the nanocomposites.

[1] Tack, J L., Ford, D.M. (2008). Thermodynamic and mechanical properties of epoxy resin DGEBF crosslinked with DETDA by molecular dynamics. *Journal of Molecular Graphics and Modelling*, 26(8), 1269-1275.

[2] Fan, H.B., Yuen, M.M. (2007). Material properties of the cross-linked epoxy resin compound predicted by molecular dynamics simulation. *Polymer*, 48(7), 2174-2178.

[3] Chen, Y., Chia, J.Y.H., Su, Z.C., Tay, T.E., Tan, V.B.C. (2013). Mechanical characterization of interfaces in epoxy-clay nanocomposites by molecular simulations. *Polymer*, 54(2), 766-773.

[4] Suter, J.L., Coveney, P.V. (2009). Computer simulation study of the materials properties of intercalated and exfoliated poly (ethylene) glycol clay nanocomposites. *Soft Matter*, 5(11), 2239-2251.

[5] Anoukou, K., Zaoui A., Zaïri F., Nait-Abdelaziz, M., Gloaguen, J.-M. (2013). Molecular dynamics study of the polymer clay nanocomposites (PCNs) : Elastic constants and basal spacing predictions,” *Computational Materials Science*, 77, 417-423.

Referee comment :

“5. What are the statistical measures for analyzing the final results?”

Author response :

It is not clear to us what referee means by this question. Molecular dynamics is a statistical mechanics technique and for the systems considered in the present study (the molecular systems 100E, N – 20E, N – 60E and N – 100E simulated at temperature conditions in the range of 300 – 600 K) all computed properties have been averaged over the configurations generated during the production phase of the simulations.

Referee comment :

“6. Page 6, line 106, does the 200 ps is sufficient ? The energy graph should be presented. Furthermore, why was this step carried out at 600 K ?”

Author response :

During the preparation and equilibration stages of the computational protocol, MD simulations have been conducted in the NVT (600 K) ensemble for 200 ps to provide sufficient kinetic energy to the system and obtain a homogeneous polymer network near the clay surface and an equilibrated state. This procedure has been adopted in previous MD studies of similar systems [1, 2, 3, 4, 5]. The plot of total energy *versus* time for the N – 100E system is reported in Fig. 1. The total energy converges quickly indicating that the system is at equilibrium within the first 100 ps.

[1] J. Suter and P. Coveney, Computer simulation study of the materials properties of intercalated and exfoliated poly (ethylene) glycol clay nanocomposites,” *Soft Matter*, vol. 5, no. 11, pp. 2239-2251, 2009.

[2] S.-C. Shiu and J.-L. Tsai, Characterizing thermal and mechanical properties of graphene/epoxy nanocomposites,” *Composites Part B : Engineering*, vol. 56, pp. 691-697, 2014.

[3] K. Anoukou, A. Zaoui, F. Zaïri, M. Nait-Abdelaziz, and J.-M. Gloaguen, Molecular dynamics study of the polymer clay nanocomposites (PCNS) : Elastic constants and basal spacing predictions,” *Computational Materials Science*, vol. 77, pp. 417-423, 2013.

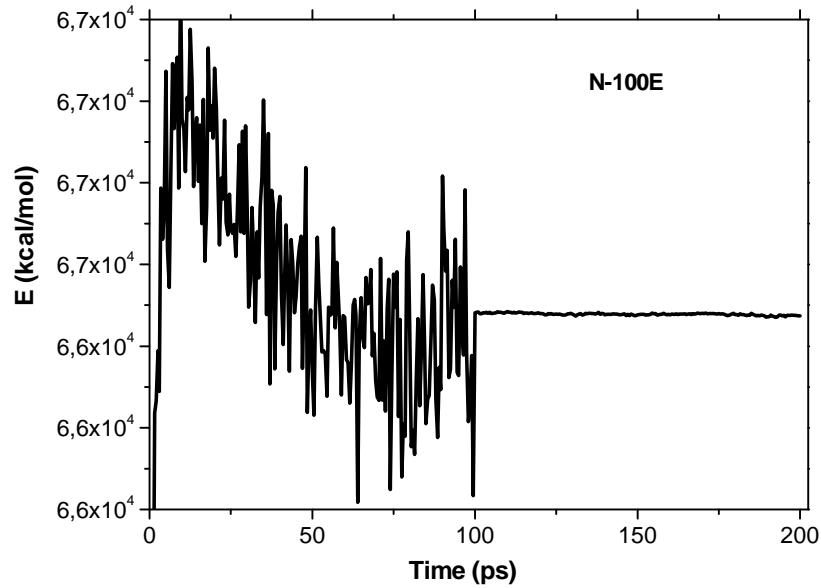


FIGURE 1 – Total energy *versus* time in NVT ensemble at 300 K for the case N – 100E. The first 100 ps correspond to the equilibration time.

[4] C. Li, A. Browning, S. Christensen, A. Strachan, Atomistic simulations on multilayer graphene reinforced epoxy composites,” *Composites Part A : Applied Science and Manufacturing*, vol. 43, no. 8, pp. 1293-1300, 2012.

[5] W. Xu, Q. Zeng, A. Yu, Young’s modulus of effective clay clusters in polymer nanocomposites, *Polymer*, vol. 53, no. 17, pp. 3735-3740, 2012.

The following paragraph has been added to the revised manuscript in section 2.3.

This procedure has been adopted in previous MD studies of similar systems [1, 2, 3, 4, 5].

Referee comment :

“7. Please, in Figure 8(b), explain the range of time that the graph has been obtained ?”

Author response :

We thank the referee for his remark and we apologize for this lack of information.

We have now added the following sentence in the revised version of manuscript to clarify this point.

To clarify this behavior, the temperature dependence of the MSD of the carbon species of pure epoxy matrix and its nanocomposites at 100 ps is reported.

We have also added the paragraph below in order to justify the typical behavior of the considered systems.

It should be emphasized that the chosen time (100 ps) for the comparison purpose may have a certain influence on the obtained results. In order to ensure the reliability of the result, other choices have also been tested (50, 150 and 200 ps) in the current work and the similar results have been observed. Thus, the reported results are the typical ones for the considered systems.

Salah NAILI,
on behalf of the authors.

1
2
3 From atomistic structure to thermodynamics and mechanical properties of
4 epoxy/clay nanocomposites: investigation by molecular dynamics
5 simulations
6
7
8

9 Van Son Vo^{a,b}, Vu-Hieu Nguyen^a, Samia Mahouche-Chergui^b, Benjamin Carbonnier^b,
10 Devis Di Tommaso^c, Salah Naili^a
11

12 ^aUniversité Paris-Est, Laboratoire Modélisation et Simulation Multi Echelle, MSME UMR 8208 CNRS, 94010
13 Créteil Cedex, France

14 ^bUniversité Paris-Est, Institut de chimie et des matériaux Paris-Est, ICMPE UMR 7182 CNRS, UPEC, 94320
15 Thiais, France

16 ^cQueen Mary, University of London, School of Biological and Chemical Sciences, Mile End Road London, E1 4NS,
17 United Kingdom
18
19
20
21

22 Abstract

23
24 Polymer/clay nanocomposites (PCNs) are multi-functional materials that have superior mechan-
25 ical and thermal properties than polymer-based materials while maintaining their characteristic
26 properties of lightweight and optical clarity. These materials are obtained by adding small amounts
27 of clay nanofillers to a polymer matrix. In this work, we proposed a molecular model to investi-
28 gate the morphology and thermomechanical properties of thermosetting clay nanocomposites. The
29 epoxy matrix was composed of several representative cross-linked epoxy units, and different struc-
30 tures of PCNs, which correspond to intercalated or exfoliated status, were considered by varying
31 the amount of polymer phase in the interlayer space. Molecular dynamics simulations of different
32 nanocomposite structures were used to provide atomistic insights into the arrangement of the con-
33 stitutive components of PCNs, the molecular interactions occurring in the interphase zone, and
34 the influence of silicate layer on the thermodynamic and elastic properties of these multi-functional
35 materials.
36
37
38
39
40
41
42
43
44

45 *Keywords:* clay, epoxy resin, exfoliated, intercalated, interphase, molecular dynamics simulations
46
47

48 1. Introduction

49
50
51
52
53
54
55
56
57
58
59
60
61
62
63
64
65

1 Polymer/clay nanocomposites (PCNs) materials are obtained by adding small amounts of clay
2 nanofillers that have an extremely high aspect-ratio (up to 0.5 μm in length and width, but only
3 1 nm in thickness) and great mechanical properties (strength and flexibility) to a polymer matrix.
4 PCNs exhibit significant enhancements in mechanical and thermal properties while maintaining

1
2
3
4 6 the characteristic of lightweight and optical clarity of polymer-based materials [1, 2, 3, 4]. To
5 7 date, the physical behavior of PCNs is not yet well understood and to the best of our knowledge,
6
7 8 few studies have considered the molecular structures and overall thermomechanical properties of
8
9 9 polymers/clay nanocomposites. So, the physical behavior of this kind of nanomaterial is not yet
10
11 well understood and still stimulate numerous research activities [5, 6].

12
13 11 The molecular structures of intercalated and exfoliated poly ϵ -caprolactone (PCL) nanocom-
14 12 posites have been previously studied by means of the molecular dynamics (MD) technique [7, 8].
15
16 13 Gardebien *et al.* [7] investigated the effect of the number and length of polymer chains on the
17
18 14 structure of intercalated nanocomposites. By examining the interlayer density profiles, the authors
19
20 15 found that the interlayer phase organizes into four layers while the charged heads of the surfactants
21
22 16 remained at the surface. On the other hand, for the exfoliated nanocomposites it was found a lay-
23
24 17 ered structure with high density of organic phase near the clay surface. The different arrangement
25
26 18 of poly (ethylene oxide) (PEO) in the intercalated and exfoliated nanocomposites was considered
27
28 19 by Suter and Coveney [9] using large-scale MD simulations, where non-modified montmorillonite
29
30 20 (MMT-Na) was used to model the inorganic phase. It was found that the PEO chains organize in
31
32 21 layers parallel to the clay surface, and because of the sodium ions and the charges within the clay
33
34 22 surface the conformation of the polymer in the exfoliated structure was significantly different from
35
36 23 the intercalated system.

37
38 24 Elastic coefficients of PCNs are important properties that can be used as parameters in con-
39
40 25 tinuum mechanical models to estimate other macroscopic properties of PCNs [10, 11]. However,
41
42 26 only Xu *et al.* [12] has used computational methods to predict the longitudinal and lateral Young's
43
44 27 *moduli* of the exfoliated and partially intercalated/exfoliated clay clusters.

45
46 28 So far, computational models of PCNs were restricted to the cases of clay with pristine surface
47
48 29 or chemically modified through cationic exchange with surfactant molecules.

49
50 30 In the works cited above, the pristine clay of organically modified clays with cationic surfactants
51
52 31 were modelled. Modification of the clay surface by the covalent grafting was, for the first time,
53
54 32 modelled using in the work of Piscitelli *et al.* [13]. Their MD simulations revealed that an increase
55
56 33 of aminosilanes concentration and the use of shorted aminosilane chains contribute to the extent
57
58 34 of the d -spacing in the clay.

1
2
3
4 35 To the best of our knowledge, there is no computational study where these silanized clays
5 36 served as fillers in polymer matrix, despite these techniques are extensively used in the synthesis
6
7 37 of epoxy/clay nanocomposites [14, 15, 16, 17, 18]. Moreover, there is only a single computational
8
9 38 study on the structural and thermosetting properties of polymer/clay nanocomposites [14], where
10
11 39 Chen and co-workers [14] considered intercalated and exfoliated clay-nanocomposites based on
12
13 40 epoxy matrix cross-linked from Diglycidyl ether of bisphenol-A and Diethylmethylenediamine
14
15 41 (DGEBA and DETDA). In this study, a series of surfactants with a single ammonium group and
16
17 42 one alkyl chain of various length were used and the failure behaviour of the interphase in terms of
18
19 43 quantifiable parameters such as peak strength, fracture energy and final separation distance were
20
21 44 determined. However, details of the molecular structures and overall thermomechanical properties
22
23 45 of these nanocomposites were not investigated.

24
25 46 In the present work, we propose a molecular model based on the epoxy-based nanocomposite
26
27 47 and silanized-clay models of Piscitelli *et al.* [13] to investigate the structural, thermodynamic and
28
29 48 mechanical properties of thermosetting clay nanocomposites. The arrangements of the constitutive
30
31 49 components of PCNs, and the effect of silicate layer on the thermodynamic and elastic properties
32
33 50 of these multifunctional materials are quantified by means of molecular dynamics simulations of
34
35 51 three nanocomposite structures consisting of different representative cross-linked epoxy molecules
36
37 52 to represent intercalated or exfoliated structures.

38
39 53 The influence of the silanized clay on the morphology and density of polymers and the molecular
40
41 54 interactions occurring at the issue of the resulting interphase region was analysed. In addition, the
42
43 55 effect of the end functional groups of the grafted aminosilane molecules, on their interactions with
44
45 56 the host epoxy polymer was also discussed by examining the local structure of nanocomposites.
46
47 57 The thermodynamics and physical properties, including the glass transition temperature, the time-
48
49 58 dependent mean squared displacement (MSD), the elasticity coefficients, and the isothermal bulk
50
51 59 *modulus* of the epoxy matrix and PCNs were also computed.

52
53 60 After this introduction on the rationale for studying the polymer/clay nanocomposites mate-
54
55 61 rials, the paper is organized as follows. In section 2, the methodology adopted to construct the
56
57 62 molecular models of sodium montmorillonite and polymer clay nanocomposites, and the force fields
58
59 63 used to conduct the molecular dynamics simulations are discussed in detail. The methods adopted
60
61 64 to determine the glass transition temperature and the mechanical properties of the PCN models
62
63
64
65

1
2
3
4 65 are also discussed in this section. The results of our simulations are presented in section 3, where
5 66 the effect of different cross-linked epoxy-units are discussed by comparing radial distribution func-
6
7 67 tion, glass transition temperatures, translational dynamics of the polymer and elastic properties.
8
9 68 Finally, in section 4, we draw the conclusion of this work.

10 11 12 69 **2. Computational Methods**

13
14
15 70 It is also important to point out that the molecular models used in this manuscript are "clay
16 71 clusters" and not true PCNs. Real PCNs should be the mixture of clay clusters with polymer
17
18 72 matrix, and they have a very complex structure [9, 19]. Therefore, a comparison with the real
19
20 73 PCNs in the experimental part will be not appropriate. Moreover, it should be noted that, in the
21
22 74 experimental part, it is impossible to make the nanocomposites with a specific controlled interlayer
23
24 75 distance. Thus, the molecular dynamics simulation has been used to investigate the properties of
25
26 76 the nanocomposites.

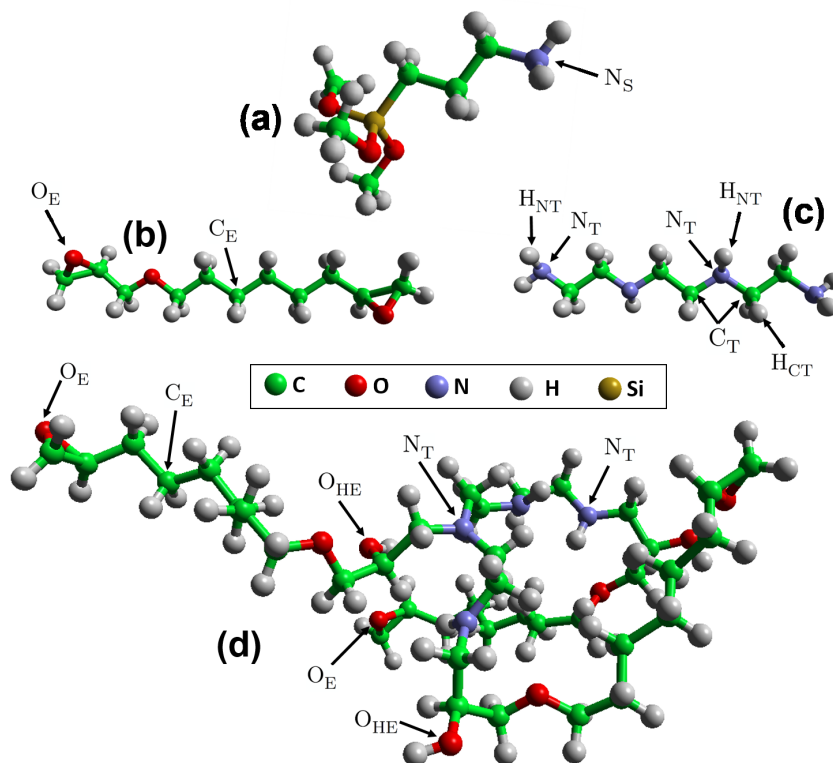
27 28 77 *2.1. Molecular model of polymer/clay nanocomposites*

29 30 78 *2.1.1. Pristine and silanized clay*

31
32 79 Let us consider a sodium montmorillonite (MMT - Na⁺) which has the chemical structure
33
34 80 Na_x(Si₈)(Al_{4-x}Mg_x)O₂₀(OH)₄ where x = 0.67 presents a cation exchange capacity of 91 meq/100g.
35
36 81 This structure corresponds to the sodium montmorillonite provided by Souther Clay Products.
37
38 82 Starting from the crystallographic unit cell [20], an orthogonal basis was defined with the Z-axis
39
40 83 being perpendicular to the clay surface of the cell. Next, the unit cell was replicated 4 times
41
42 84 according to the X-axis and 3 times according to the Y-axis. Then, 8 atoms of Al³⁺ were randomly
43
44 85 chosen and replaced by Mg²⁺ in the octahedral layer, which resulted in a charge deficiency of -8
45
46 86 for the clay layer. Finally, 8 sodium ions Na⁺ were added in the interlayer space to obtain the
47
48 87 complete MMT - Na⁺ cell. The size of the MMT - Na⁺ cell were 21.12 × 27.42 × 6.56 Å³.

48 88 For the silanized clay, the size along the Z-axis of the MMT - Na⁺ cell was fixed at 18 Å,
49
50 89 which corresponds to the bilayer organization of aminosilanes within the clay interlayer space
51
52 90 [21, 16, 17, 13, 22]. Grafting of aminosilanes onto the clay surface was carried out following the
53
54 91 procedure proposed by Piscitelli *et al.* [13]. Herein, it is assumed that the silane molecules can be
55
56 92 grafted covalently with the oxygen atoms on the surface of clay [13]. We only considered the case
57
58 93 where the 3-aminopropyltrimethoxysilane molecules were linked with clay surface through three

1
2
3
4 94 covalent bonds [13]. The molecular structure of this aminosilane molecule is shown in Fig. 1(a). In
5
6 95 this model, 8 aminosilanes were grafted on each clay surface. This corresponds to the number of
7
8 96 monocationic surfactant needed to obtain a fully treated clay surface based on its cation-exchange
9
10 capacity.

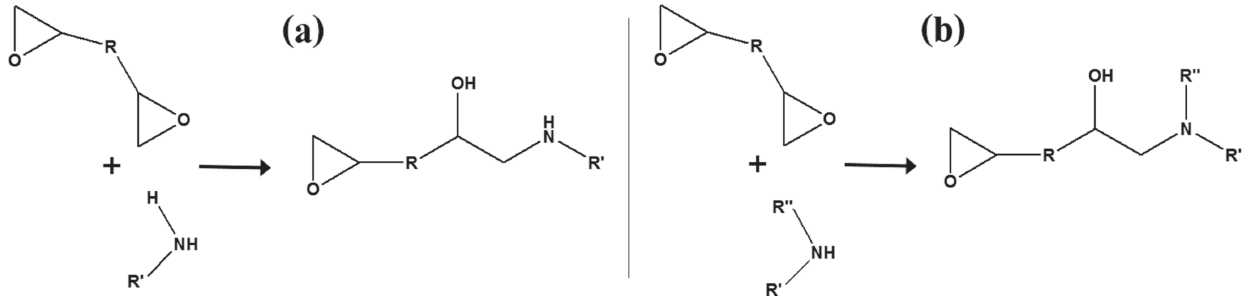


11
12
13
14
15
16
17
18
19
20
21
22
23
24
25
26
27
28
29
30
31
32
33
34
35
36
37
38
39 Figure 1: The molecular structure of (a) aminosilane molecule, (b) epoxy monomer molecule, (c) amine-based
40
41 hardener molecule and (d) the representative cross-linked molecule. The cross-linked molecule (d) is obtained from
42
43 the cross-linking reaction between three epoxy monomers (b) and one hardener (c).
44
45
46

47 98 *2.1.2. Polymer clay nanocomposites*

48
49 99 In our PCN model, the polymer matrix consists of representative cross-linked molecules as
50
51 100 shown in Fig. 1(d). This type of cross-linked molecules has been previously used for simulating
52
53 101 thermoset polymers [23, 24, 25, 26]. The use of these representative cross-linked molecules was
54
55 102 also shown to be suitable for estimating thermodynamic and mechanical properties of thermoset
56
57 103 polymer [27]. Figure 2 reports the curing reaction mechanism between the epoxy group and the

1
2
3
4 104 primary amine group. The carbon-oxygen bond in the epoxy monomers is broken through opening
5 105 of the epoxy ring. The oxygen-end of the opened epoxy ring takes over the hydrogen atom from
6
7 106 a nearby amine group in the hardener molecule and leaves a dangling nitrogen in the hardener
8
9 107 molecule, which forms a covalent bond with the carbon-end of the opened epoxy ring. This process
10
11 108 allows the epoxy monomer to link to an amine based hardener.



24 Figure 2: Curing reaction between the epoxy resin and (a) primary amine or (b) secondary amine of hardener.

27
28 109 The structures of the epoxy monomer and of the hardener used in this work are reported in
29
30 110 Fig. 1(b) and (c), respectively. Each epoxy monomer has two reactive epoxy groups and the hard-
31
32 111 ener has six reactive amine groups. The representative cross-linked molecule was build from the
33
34 112 cross-link process between three linear epoxy monomers and one chain of curing agent. Therefore,
35
36 113 as suggested in the work of Yu *et al.* [27], a cross-linking ratio of 50 % is used for this repre-
37
38 114 sentative molecule based on the consummation of the reactive functions on both epoxy monomer
39
40 115 and hardener molecules. Figure 1(d) shows the configuration of the representative cross-linked
41
42 116 molecule.

43
44 117 The procedure used to build the nanocomposite structures from the organically modified clay
45
46 118 followed the work of Anoukou *et al.* [19]. Firstly, the silanized system was relaxed in NVE (constant
47
48 119 Number, Volume and Energy) ensemble for 200 ps. Then, the simulation cell was replicated 2 times
49
50 120 in both X- and Y-axes in order to have enough surface before adding the representative cross-linked
51
52 121 molecules. As a consequence, its surface dimensions became $42.24 \times 54.84 \text{ \AA}^2$ in the XY-plane
53
54 122 geometry. The size of the c-cell (Z-direction) of the simulation box was shifted to insert the
55
56 123 cross-linked molecules in the interlayer space. Three PCNs containing 20, 60 and 100 cross-linked
57
58 124 molecules (denoted by (N - 20E), (N - 60E) and (N - 100E)) which correspond to three [interlayer](#)
59
60 125 [distances](#). For the purpose of comparison, a model that contains only cross-linked molecules (100

1
2
3
4 126 molecules), designated as pure epoxy, was also built. Note that the orthorhombic symmetry was
5 127 assumed for all molecular systems in this study. The orthorhombic symmetry corresponds to
6
7 128 $\alpha = \beta = \gamma = 90^\circ$, where the three angles α, β and γ are the angles between the Y- and Z-axes,
8
9 129 between the X- and Z-axes, and between the X- and Y-axes, respectively. The initial structures of
10
11 130 the aminosilane and cross-linked molecules were generated by using the Aten package [28].

13 131 *2.2. Force fields description*

15 132 Electrostatic charges and interatomic potential parameters for all atoms in the montmoril-
16 133 lonite layer MMT – Na⁺ were taken from CLAYFF [29]. For the organic phase, the molecular
17 134 structures and Mulliken charges of organosilane and cross-linked molecules were optimized at the
18 135 B3LYP/6 – 311⁺⁺G* level using the Gaussian 09 program [30]. For the organic phase, the geome-
19 136 tries of both organosilane and cross-linked molecules were optimized by using the DFT method at
20 137 B3LYP/6 – 311⁺⁺G* level implemented in Gaussian 09 program [30]. The electrostatic charges
21 138 of these optimized molecules were calculated at B3LYP/6 – 311⁺⁺G** level by using the mul-
22 139 liken population analysis. The potential parameters for the organic phase were taken from the
23 140 INTERFACE-FF force field [31]. In particular, we used the 12-6 van der Waals (vdW) form in-
24 141 stead of 9-6 vdW in the INTERFACE-FF for polymer and aminosilan molecules as described in
25 142 the conversion method presented by Heinz *et al.* [31]. The FIELD file for the DL_POLY molecular
26 143 dynamics code was generated using the DL_FIELD program [32].

27
28
29
30 144 Given that the CLAYFF force field has been previously adopted to calculate the structural and
31 145 mechanical properties of clays and other PCNs systems [33, 34, 19, 9, 35], given that CLAYFF
32 146 has a rather simple functional form, which makes this force field computationally fast and robust
33 147 for the simulation of multicomponent complex systems, CLAYFF is a suitable potential model to
34 148 accurately simulate the structural and thermodynamic properties of epoxy/clay nanocomposite. It
35 149 was previously pointed out that this force field is not appropriate to compute cleavage and binding
36 150 energies [36, 37, 38], but the evaluation of these properties is not the focus of the present study.

50 151 *2.3. Molecular dynamics simulation procedure*

52 152 The molecular dynamics (MD) simulations were performed using DL_POLY 4.5 [39]. The in-
53 153 tegration algorithms were based on a Verlet leap-frog scheme. Periodic boundary conditions were
54 154 applied to three directions of the simulation box. The Nosé-Hoover algorithm was used to control

1
2
3
4 155 the temperature and pressure of molecular systems. The long-range electrostatic interactions be-
5 156 tween the charges of all species were computed using the Smoothed Particle Mesh Ewald (SPME)
6
7 157 method with the relative error of 10^{-6} [40]. The time step of 0.5 fs was chosen for all MD simu-
8
9 158 lations to maintain the system stability. The system properties were recorded every 5 fs, whereas
10
11 159 the mean square displacements of atoms were recorded every 2 ps.

12
13 160 The molecular system were sequentially simulated in two types of thermodynamic ensembles,
14 161 NVT (constant Number, Volume and Temperature) and NPT (constant Number, Pressure and
15
16 162 Temperature). At first, simulations in the NVT ensemble at 600 K and 200 ps were carried
17
18 163 out. The objective of this step is to provide a sufficient kinetic energy to the cross-linked epoxy
19
20 164 molecules, so that the homogeneous polymer layers can be achieved near the clay surface. Then,
21 165 the MD simulations in NVT ensemble were conducted at 300 K for another 200 ps. After this
22
23 166 step, the size according to Z-axis of the simulation box was adjusted by removing the empty space
24
25 167 between the clay layers in order to approach the equilibrium configuration of the molecular systems.
26
27 168 This procedure has been adopted in previous MD studies of similar systems [9, 25, 19, 24, 12].

28
29 169 Simulations in the NPT ensemble with $P = 0$ atm and $T = 300$ K were then conducted
30
31 170 for 500 ps in order to equilibrate the volume of the unit cell and ring the system in a stress-
32 171 free state [25]. The production stage of the simulations was carried out in NPT ensemble at room
33
34 172 temperature (300 K) and atmospheric pressure (1 atm) for 2000 ps. During the simulation process,
35
36 173 the positions of the atoms in two silicate layers were kept fixed whereas the atoms in all organic
37
38 174 components were free to move. The stabilization of the total energy, pressure and temperature
39 175 of the molecular system was monitored to ensure that the system was at equilibrium during the
40
41 176 production phase of the MD simulations. The configurations at equilibrium state of the pure epoxy
42
43 177 matrix (N – 20E) and of the nanocomposites ((N – 20E), (N – 60E) and (N – 100E)) are shown in
44
45 178 Fig. 3. The interlayer distance d -spacing is 3.01, 5.57 and 7.77 nm respectively (see Tab. 1). The
46
47 179 density of all molecular systems at the equilibrium state is also reported in Tab. 1.

49 180 2.4. Determination of glass transition temperature

51 181 At the glass transition temperature T_g , the polymer changes from a ‘glassy’ state (an amorphous
52 182 solid trapped in a non-equilibrium state) to a rubber (for cross-linked systems over the gel point)
53
54 183 or liquid (when chains are not covalently bonded to each other as in the thermoplastics) state
55
56
57 184 [41]. For a molecular system, the value of T_g is defined by the temperature at which the density-

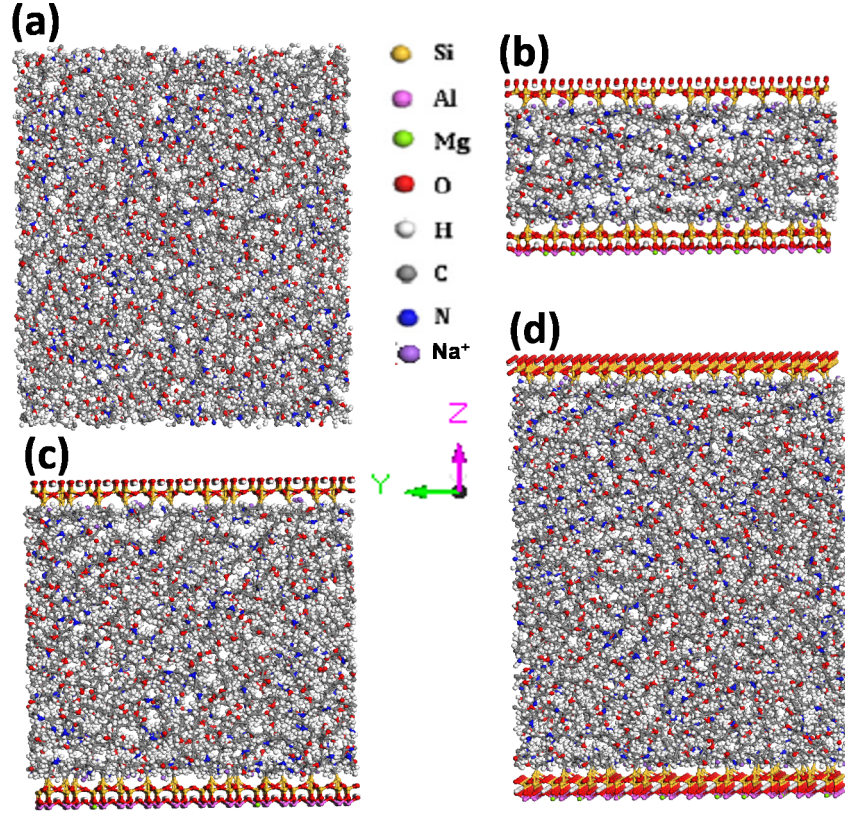


Figure 3: The configuration at equilibrated state of (a) pure epoxy matrix 100E, (b) nanocomposite containing 20 representative molecules ($N - 20E$), (c) nanocomposite containing containing 60 representative molecules ($N - 60E$) and (d) nanocomposite containing 100 representative molecules ($N - 100E$).

temperature relation becomes discontinued. At the transition temperature, the motion of polymer chain segments increases significantly and the mechanical properties of polymers become very different from those below the value of T_g . The value of the transition temperature T_g is governed by local chain dynamics and represents an intrinsic signature of the molecular structure [41].

The determination of T_g was performed by varying the system temperature from 300 K to 500 K at a constant heating rate of 20 K/500 ps and at the pressure $P = 1$ atm. At each temperature, the density was only averaged over the last 200 ps.

Besides of using the density-temperature relationship, the quantity T_g can also be obtained from the mean squared displacement-temperature relationship of some typical atom types where the mean squared displacement (MSD) stands the time-dependent.

1
2
3
4 195 *2.5. Determination of mechanical properties*

5
6 196 In this work, the elastic properties of the PCNs considered were quantified using the strain
7
8 197 fluctuations method proposed by Parrinello and Rahman [42], which was then further developed
9
10 198 in the work of Ray [15], and Van Workum and de Pablo [43]. This approach allows to determine
11
12 199 the elasticity properties of a molecular system from using a single MD simulation. Particularly,
13
14 200 the elasticity properties of the system can be determined at a specific temperature [35]. This is
15
16 201 particularly important for the polymeric materials because their mechanical behaviours strongly
17
18 202 depend on the temperature.

19
20 In order to perform the MD calculation with strain fluctuations method, the equilibrated sys-
21
22 tems obtained in NPT ensemble were used as describe in the section 2.3. It is worth noting that
23
24 at this step, all atoms were free to move. During the simulation, the system was subjected to a
25
26 three-dimensional stress field in the $N\sigma T$ ensemble (constant Number, Stress and Temperature).
27
28 The obtained strain field was determined in each case of temperatures. The components of the
29
30 4-th order effective compliance tensor s_{ijkl} of the considered molecular system are given by:

$$s_{ijkl} = \frac{\langle V \rangle}{K_b T} (\langle \epsilon_{ij} \epsilon_{kl} \rangle - \langle \epsilon_{ij} \rangle \langle \epsilon_{kl} \rangle), \quad (1)$$

31
32 203 where K_b , ϵ_{ij} , T and V are the Boltzmann constant, the components of strain tensor, the imposed
33
34 204 temperature and the volume of the molecular system, respectively. The angular brackets $\langle \star \rangle$
35
36 205 designates the ensemble average of the cell volume. Each index varies from 1 to 3, where each
37
38 206 value of these indexes 1, 2 and 3 is associated with the X-axis, Y-axis and Z-axis, respectively. The
39
40 207 stiffness tensor \mathfrak{c} can be then computed according to the relation $\mathfrak{s}^{-1} = \mathfrak{c}$ whose the components
41
42 208 are given by s_{ijkl} .

43
44 209 To determine the isothermal bulk *modulus* κ_T , the temperature was set at the temperature
45
46 210 $T = 300$ K and MD simulations were conducted in NPT ensemble with different values of the
47
48 211 pressure in range 0.1 MPa (*i.e.* $P = 1$ atm) to 2.5 GPa (*i.e.* $P = 25$ katm) [19]. Each simulation
49
50 212 was carried out for 500 ps and the average volume was taken for the last 200 ps.

51
52 The bulk *modulus* κ_T is related with the compressibility of the substance. It is defined as the
53
54 ratio of the infinitesimal pressure increase to the resulting relative decrease of the volume. As a
55
56 consequence, the bulk *modulus* κ_T at temperature T is determined by using a relationship between
57
58
59
60
61
62
63
64
65

1
2
3 P and V as follows [19]:
4
5

$$\kappa_T = -V \left(\frac{\partial P}{\partial V} \right)_T, \quad (2)$$

6
7
8
9 213 where P is pressure, V is volume, and $(\partial P/\partial V)_T$ denotes the partial derivative of pressure with
10 214 respect to volume at constant temperature T .
11
12

13 14 215 **3. Results and discussion**

15 16 216 *3.1. Structural characterization of PCNs*

17 18 217 *3.1.1. Density distribution profiles*

19
20 218 Figure 4 compares the density profiles of pure epoxy matrix and different nanocomposite sys-
21 219 tems at room temperature (*i.e.* $T = 300$ K). The position $z = 0$ along the Z-axis corresponds to
22 220 the median plane of the simulation box, whereas the two dash lines present the positions of clay
23 221 surfaces. The positions of clay surfaces were determined from the density profile of surface oxygen
24 222 atoms of silicate layer.
25
26
27

28
29 223 In the pure epoxy matrix system (see Fig. 4(a)) the density profile of polymer is almost con-
30 224 stant along the Z-axis with a mean value $d_m = 1.038 \text{ g} \cdot \text{cm}^{-3}$, which is similar to the values
31 225 derived from the diglycidyl ether of bisphenol F (DGEBF) cross-linked with curing agent diethyl-
32 226 toluenediamine (DETDA) ($d_m = 1.07 - 1.075 \text{ g} \cdot \text{cm}^{-3}$ given by Tack and Ford [44]) and from the
33 227 epoxy network composed of EPON 862 epoxy resin and triethylenetetramine (TETA) curing agent
34 228 ($d_m = 1.08 \text{ g} \cdot \text{cm}^{-3}$, given by Fan and Yuen [45]). These values are slightly smaller than the
35 229 ones obtained by experimental measurements of epoxy networks ($d_m = 1.13 \text{ g} \cdot \text{cm}^{-3}$ in [46], or
36 230 $d_m = 1.16 \text{ g} \cdot \text{cm}^{-3}$ in [47]). The experimental density of epoxy cross-linked matrix was determined
37 231 using fully cross-linked epoxy resin whereas in this study, to reduce the computational cost, a low
38 232 cross-link density has been adopted. The difference between the result obtained herein and the
39 233 ones presented in the other works may be associated to the small cross-link density, the type of
40 234 epoxy and hardener, or the force field adopted in this study [44, 23, 48, 49].
41
42
43
44
45
46
47
48

49 235 Significant variations of the density profiles are observed in Figs. 4(b), (c) and (d) indicating
50 236 the influence of silicate layers on the molecular configuration of the epoxy matrix. In all three
51 237 nanocomposite structures, the confined polymer region near the clay surface becomes similar to a
52 238 layered structure with the density much higher than the density of the bulk polymer.
53
54
55
56
57
58

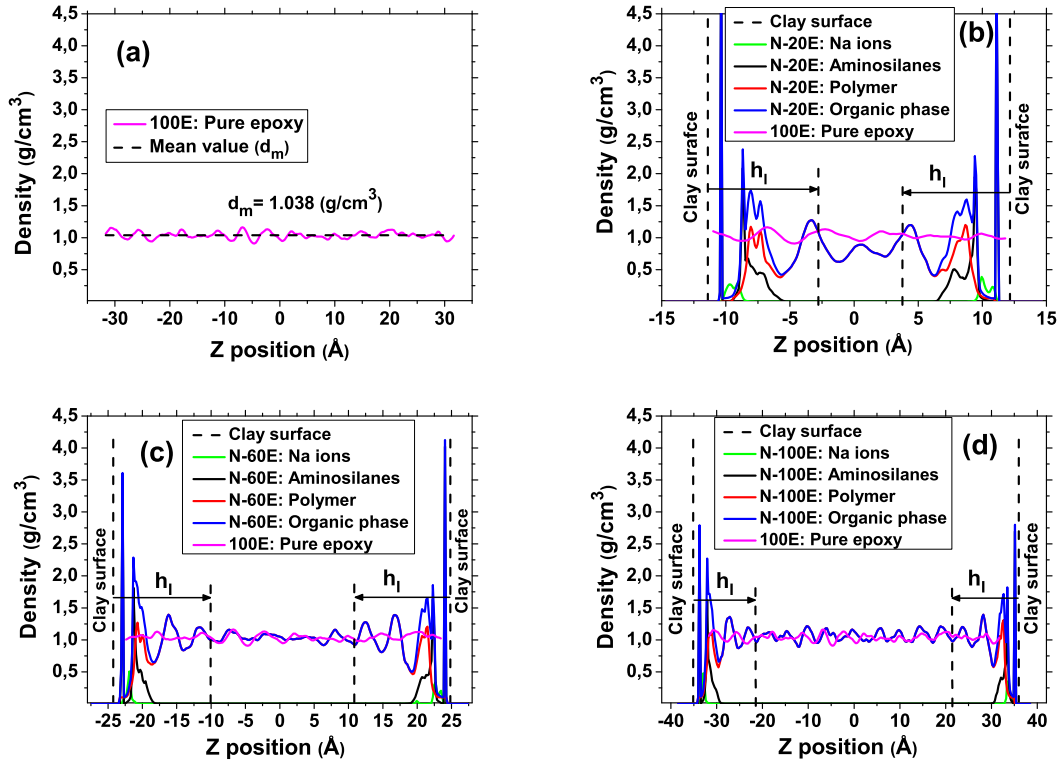


Figure 4: Density profiles of the different simulated systems: (a) Pure epoxy matrix containing 100 representative molecules, (b) Nanocomposite containing 20 representative molecules (N – 20E), (c) Nanocomposite containing 60 representative molecules (N – 60E), (d) Nanocomposite containing 100 representative molecules (N – 100E). For the purpose of comparison, the density profile of the pure epoxy matrix is put together with that one of nanocomposite.

Our results are similar to other MD simulations of poly ϵ -caprolactone/clay nanocomposites [9] and the graphene/epoxy nanocomposites [25, 24, 50]. In particular, Suter and Coveney [9] suggested that the high density of organic phase in the region close to the clay surface shows a strong affinity between the polymer matrix and the clay platelets.

On contrary, by studying epoxy/clay nanocomposite models using MD simulations, Chen *et al.* [14] have shown that the density of epoxy resin near clay surface is slightly lower than that of bulk matrix. Moreover, no layering configuration has clearly been observed. This may be explained in terms of different models used for the surfactants. In fact, in our model, the grafted aminosilanes have reactive amino functions NH_2 to epoxy matrix, whereas in [14], different organic molecules composed of a single ammonium head group NH_3^+ and one alkyl chain of various lengths C_n have

1
2
3
4 249 been used.

5 250 Therefore, one may suggest that the presence of the reactive functions NH_2 on the grafted
6
7 251 aminosilanes is the main cause of the high density of organic phase near the clay surface. As
8
9 252 a consequence, this interphase may enhance the mechanical properties as well as the adhesion
10
11 253 between the clay layer and polymer matrix, in agreement with what suggested in previous works
12
13 254 [21, 17].

14 255 Besides, the results show that aminosilane molecules are always found in the range $[0, 7]$ Å
15
16 256 from the clay surface thanks to its covalent bonds with clay surface. Moreover, all sodium ions are
17
18 257 close to clay surface due to its strong electrostatic interactions with the negatively charged silicate
19
20 258 layer. From the density profile of nanocomposite structures, we can also estimate the thickness of
21
22 259 interphase region [12, 51]. In Fig. 4, it can be observed that the thickness of the interphase of the
23
24 260 exfoliated (N – 100E) or nearly exfoliated structures (N – 60E) is approximately 15 Å. For the
25
26 261 intercalated structure (N – 20E), only a 10 Å thickness interphase layer was found.

27 262 The density profiles in three nanocomposite structures are presented in Figs. 4(b), (c) and
28
29 263 (d). For the intercalated structure (N – 20E), the density of interlayer epoxy resin ($0.77 \text{ g} \cdot \text{cm}^{-3}$)
30
31 264 is smaller than the bulk epoxy matrix ($1.038 \text{ g} \cdot \text{cm}^{-3}$). This result is similar to the one given
32
33 265 by Chen *et al.* [14] who found an average density of $0.76 \text{ g} \cdot \text{cm}^{-3}$ for organic phase in case of
34
35 266 intercalated nanocomposite, and may be explained by strong confined effects in the narrow space
36
37 267 between silicate layers, particularly for non-flexible polymers as epoxy resins [14].

38 268 When the number of representative molecules increases, the configuration of nanocomposite
39
40 269 structures changes from intercalated to the exfoliated one. In Figs. 4(c) and (d), one may observe
41
42 270 that the density of polymer matrix in the region far away from the clay surface tends to that of the
43
44 271 bulk polymer matrix. Compared to the intercalated structure, in the exfoliated systems (N – 60E
45
46 272 and N – 100E), individual silicate layers with reactive surface may locally reinforce the interphase
47
48 273 while maintaining the behavior of bulk polymer matrix for the confined polymer.

49 274 3.2. Radial distribution function

50
51 275 The radial distribution function (RDF), denoted by $g(r)$, is defined as the probability of finding
52
53 276 a given particle at a distance r from a reference particle. In this work, the radial distribution
54
55 277 functions were studied in order to better understand the short- and medium-range structure in
56
57 278 PCNs.

279 For the pure epoxy matrix, which is composed of numerous cross-linked representative molecules,
 280 Fig. 5(a) compares the RDF of the reactive oxygen atoms in epoxy functions with other atom types
 281 in the hardener backbone, such as the reactive nitrogen N_T , the hydrogen linked to nitrogen H_{NT} ,
 282 the carbon C_T and the hydrogen linked to carbon H_{CT} (see Fig. 1).

283 There are two peaks at approximately 2 Å and 3 Å that correspond to the short-range interac-
 284 tion between $O_E - N_T$ and $O_E - H_{NT}$ atoms, respectively. The RDFs between the oxygen atoms in
 285 epoxy with the carbon (C_T) and hydrogen (H_{CT}) atoms do not display peaks at distance lower than
 286 3.5 Å. The peaks smaller than 3.5 Å in the RDF curves are mainly due to hydrogen and chemical
 287 bonds between atoms, whilst those beyond 3.5 Å correspond to van der Waals and electrostatic
 288 interactions. Thus, small distances between these reactive atoms show their tendency to cross-link
 289 together. In fact, by checking the close contact between these pairs of reactive atoms, several
 290 authors suggested the formation of the cross-linking between the epoxy resin and the hardener
 291 [52, 48, 53, 54]. Besides, some small peaks within the range [4, 7] Å could contribute to the inter-
 292 or intra-molecular RDF of the cross-linked representative molecules. The case with the nearly
 293 exfoliated structure (N – 60E) is reported in Fig. 5(b) showing the analogous RDF profiles at the
 294 ones found for epoxy matrices in PCN structures.

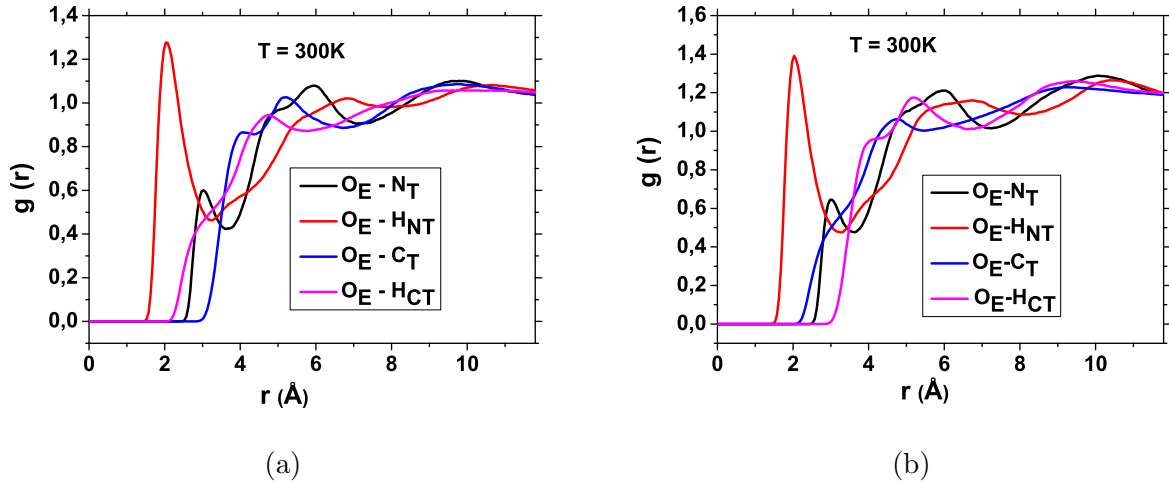


Figure 5: RDF's of reactive oxygen atoms in epoxy functions (O_E) to other atoms in hardener backbone such as reactive nitrogen N_T , hydrogen linked to nitrogen H_{NT} , carbon C_T and hydrogen linked to carbon H_{CT} of two cases (a) pure epoxy matrix and (b) a nanocomposite that contains 60 epoxy representative molecules.

295 The local interactions between the confined polymer matrix and the grafted aminosilanes were

1
2
3
4
5
6
7
8
9
10
11
12
13
14
15
16
17
18
19
20
21
22
23
24
25
26
27
28
29
30
31
32
33
34
35
36
37
38
39
40
41
42
43
44
45
46
47
48
49
50
51
52
53
54
55
56
57
58
59
60
61
62
63
64
65

296 also quantified in terms of the RDF profiles. The RDFs of reactive nitrogen atoms of grafted
 297 aminosilanes N_S to some typical atoms in cross-linked representative molecules such as O_E , C_E ,
 298 C_T and N_T are reported in Fig. 6, where an intense peak at 3 Å can be seen in the N_S - O_E RDF
 299 indicating a strong interaction between the nitrogen atoms of primary amine functions N_S on the
 300 grafted aminosilanes and the oxygen atoms in epoxy groups O_E . The profile of this peak is similar to
 301 the one of $O_E - N_T$ in pure epoxy matrix presented in Fig. 5(a). A peak located at 3 Å between the
 302 N_S atoms of the grafted aminosilanes and the N_T atoms of the cross-linked molecule is associated
 303 to the hydrogen bonding between two amine groups. In summary, these RDF's profiles show a
 304 strong affinity between the grafted aminosilanes and the cross-linked polymer matrix.

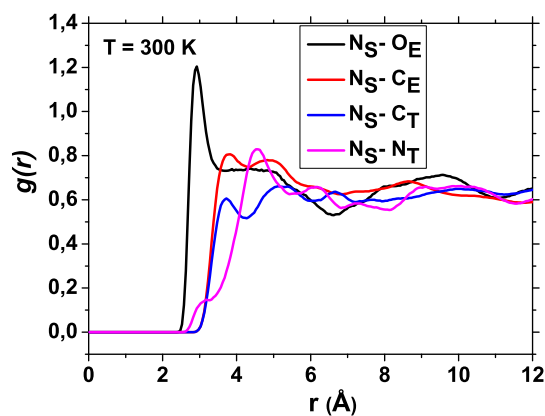
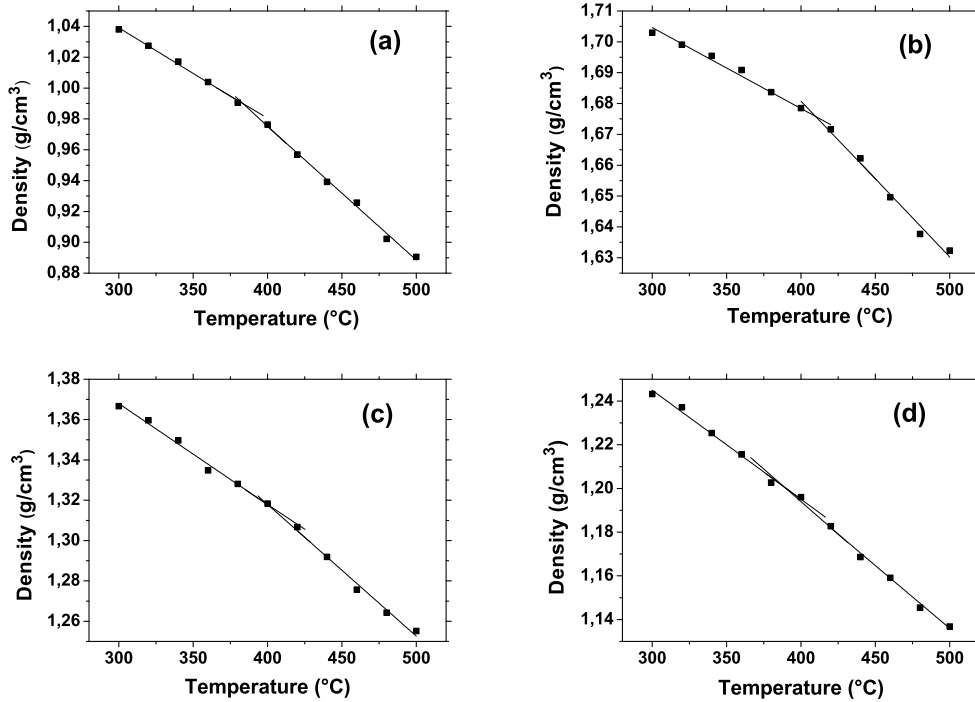


Figure 6: RDF's of reactive nitrogen atoms in surfactant (N_S) to other atoms in the cross-linked representative molecule such as reactive oxygen O_E , carbon in epoxy backbone C_E , carbon in hardener backbone C_T , reactive nitrogen in hardener backbone N_T ,

3.3. Glass transition temperature

Figure 7(a) shows the variation of the density of pure epoxy matrix and its nanocomposites as a function of temperature. For all systems, the density decreases with increasing temperature and there are two linear regions, which correspond to the glass and rubber states of the polymeric material, respectively. The abscissa of the intersection of two linear curves, which are obtained by taking a linear fitting of the data, corresponds to T_g . As the value of T_g is somewhat dependent on the method and number of data used for the linear regression fitting, here we report the temperature range where there is a slope change. Therefore, it is more suitable to take into account a range of

1
2
3
4 313 temperature in which there is a slope's change. For the pure epoxy matrix, T_g was found in the
5 314 range [380, 385] K, which is in line with the results reported in several other MD works of epoxy
6
7 315 matrix [45, 55, 56, 25, 57].
8
9



10
11
12
13
14
15
16
17
18
19
20
21
22
23
24
25
26
27
28
29
30
31
32
33
34
35 Figure 7: Plots of unit cell density of MD simulation versus temperature used to estimate the glass transition
36 temperature T_g for epoxy and epoxy/clay nanocomposites: (a) pure epoxy matrix, (b) nanocomposite containing
37 20 representative molecules (N20 – E), (c) nanocomposite containing 60 representative molecules (N60 – E), (d)
38 nanocomposite containing 100 representative molecules (N100 – E).
39
40
41

42
43 316 The results shown in Fig. 7(b), (c) and (d) highlight the effect of clay layers on the glass
44 317 transition temperature T_g of the epoxy matrix. The intercalated structure (N – 20E) has the
45 318 largest glass transition temperature T_g , which is in the range [415, 425] K. The glass transition
46 319 temperature decreases when the number of cross-linked epoxy molecules increases, with values
47 320 in the range [395, 415] K for (N – 60E) and in the range [385, 395] K for (N – 100E) systems,
48 321 respectively. The exfoliated structure (N – 100E) and pure epoxy matrix have very similar T_g
49 322 values.
50
51
52
53

54
55 323 This result can be explained in terms of the few polymer molecules inserted into the interlayer
56 324 space in the (N20 – E) system, where all polymer molecules are located close to the clay surfaces
57
58
59
60
61
62
63
64
65

1
2
3
4 325 and the grafted aminosilanes. These polymer molecules strongly interact with the reactive grafted
5 326 aminosilanes as well as the clay surfaces as shown by the RDF profiles in Figs 5 and 6 and con-
6
7 327 sequently the mobility of the polymer is reduced. As the number of cross-linked molecules in the
8
9 328 three PCNs increases on going from (N – 20E) to (N – 100E) then the proportion of polymer
10
11 329 molecules that do not interact with the surface decreases, and the thermodynamic behaviour tends
12
13 330 to that of the bulk polymer matrix.

14 15 331 *3.4. Translational dynamics of polymer*

16 332 The translational dynamics of polymer in pure epoxy matrix and its nanocomposites have been
17
18 333 quantified in terms of the mean square displacement of the carbon atoms in the epoxy backbone.
19
20 334 Figure 8(a) reports the MSD of the C species along the MD trajectories in the temperature range
21
22 335 [300, 480] K for the nanocomposite containing 100 cross-linked molecules (N – 100E). As expected,
23
24 336 diffusional behaviour consistently increases with temperature. Moreover, the mobility of the carbon
25
26 337 atoms in epoxy backbone, and consequently the polymer, shows transitional behaviour as a function
27
28 338 of temperature.

29 339 To clarify this behavior, the temperature dependence of the MSD of the carbon species of pure
30
31 340 epoxy matrix and its nanocomposites at 100 ps is reported. As can be seen from the Fig. 8(b),
32
33 341 a gradual change in the MSD value of the pure epoxy matrix is found at around 380 K, whereas
34
35 342 it becomes bigger for all nanocomposite structures. The intercalated structure (N – 20E), which
36
37 343 shows the highest T_g due to the stronger interaction with the clay surface, is characterized by the
38
39 344 slowest increase of MSD with the temperature. Particularly, it is observed that the MSD value of
40
41 345 the pure epoxy quickly increases once the glass transition temperature has been reached. From
42
43 346 these observed behaviour on the glass transition temperature, it is possible to conclude that the
44
45 347 addition of reactive clay significantly enhances the thermal stability of epoxy-based materials. **It**
46
47 348 **should be emphasized that the chosen time (100 ps) for the comparison purpose may have a certain**
48
49 349 **influence on the obtained results. In order to ensure the reliability of the result, other choices have**
50
51 350 **also been tested (50, 150 and 200 ps) in the current work and the similar results have been observed.**
52
53 351 **Thus, the reported results are the typical ones for the considered systems.**

54 352 *3.5. Bulk modulus*

55 353 The isothermal bulk *modulus* of pure epoxy system and nanocomposites determined using
56
57 354 Eq. (2) are reported in Tab. 1. The isothermal bulk *modulus* of the pure epoxy matrix is larger

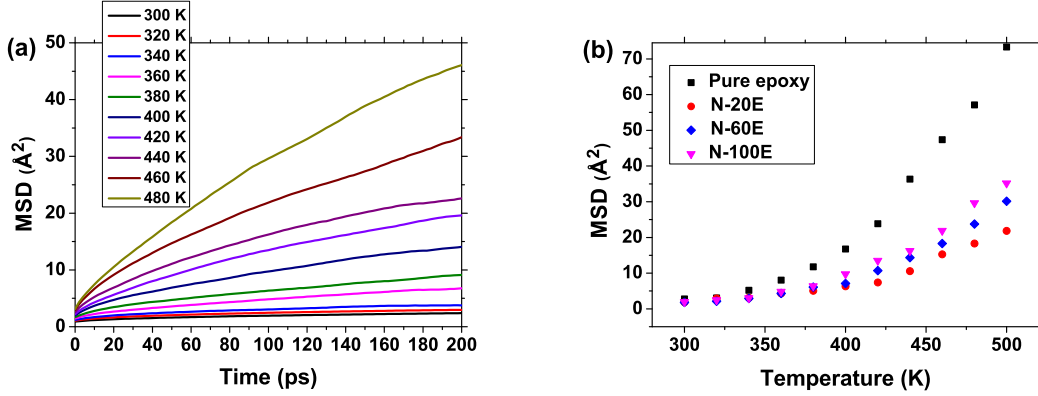


Figure 8: Mean square displacement of carbon atoms in the backbone of cross-linked molecules: (a) case of a nanocomposite containing 100 representative molecules (N – 100E) at different temperatures; (b) pure epoxy and its nanocomposites at $t = 100$ ps.

than the bulk *moduli* computed for the nanocomposite structures. There is a slight difference between κ_T for (N – 60E) and (N – 100E). The bulk *modulus* of (N – 20E) structure is significantly smaller than the ones obtained for (N – 60E) and (N – 100E) as well as the pure epoxy. Note that the isothermal bulk *modulus* represents the volume variation of the molecular system with respect to the pressure. This volume variation mainly depends on changes of the organic phase volume and density. A small volume of organic phase in the intercalated structure is likely to be the reason for the observed results.

Table 1: Physical and structural properties of several molecular systems at 300 K determined by using MD simulations. κ_T is the isothermal bulk *modulus*.

Molecular systems	κ_T (GPa)	Density (g/cm ³)	d_{001} (nm)
Pure epoxy 100E	15.65	1.038	–
(N – 100E)	15.28	1.24	7.77
(N – 60E)	15.05	1.37	5.57
(N – 20E)	12.20	1.70	3.01

362 3.6. Elasticity coefficients

The elasticity properties of the pure epoxy matrix and its nanocomposites at various temperatures were computed using the strain fluctuations method (see Eq. (1)). The 4-th order tensors in three dimensions can be represented in a Euclidian six-dimensional space as (6×6) matrices. To this end, the representation adopted in this work is called the *Voigt's* representation in which the new indexes I and J vary in the set $\{1, \dots, 6\}$ such as $I = (i, j)$ and $J = (k, l)$, where the indices i, j, k and l vary in the set $\{1, \dots, 3\}$. The relation between these indices is the following $1 = (1, 1), 2 = (2, 2), 3 = (3, 3), 4 = (2, 3), 5 = (1, 3)$ and $6 = (1, 2)$. So, the the relation between symmetric matrix \mathbf{C} with the 4-th order tensor \mathbf{c} , whose the components are c_{ijkl} is given by these components:

$$C_{IJ} = c_{ijkl}. \quad (3)$$

Table 2: The elastic constants (in GPa) at various temperature conditions

Molecular systems	Temperature	C_{11}	C_{22}	C_{33}	C_{12}	C_{13}	C_{23}	C_{44}	C_{55}	C_{66}
Pure epoxy	(300 K)	3.38	3.46	3.28	2.52	2.18	1.93	1.69	2.28	1.84
Pure epoxy	(350 K)	1.97	1.83	1.87	1.56	1.51	1.43	0.98	0.685	0.818
Pure epoxy	(400 K)	0.84	0.75	0.70	0.66	0.54	0.52	0.20	0.25	0.49
(N – 100E)	(300 K)	39.5	38.2	4.37	17.3	3.2	2.82	2.77	2.33	32.3
(N – 100E)	(350 K)	37.06	32.96	3.39	15.82	2.85	3.65	1.40	1.32	26.46
(N – 100E)	(400 K)	24.1	25.47	1.49	11.11	1.02	0.77	0.26	0.49	19.66
(N – 60E)	(300 K)	59.8	60.2	5.26	24.3	1.9	2.2	1.93	3.85	49.2
(N – 60E)	(350 K)	46.1	56.2	3.13	27.0	1.23	0.93	1.03	1.46	49.1
(N – 60E)	(400 K)	31.2	39.8	1.87	15.9	1.1	1.31	0.534	0.586	33.6
(N – 20E)	(300 K)	127	122	3.77	48.5	2.39	2.68	5.63	2.44	117
(N – 20E)	(350 K)	106	113	3.70	47.90	1.50	1.15	3.21	2.78	92.10
(N – 20E)	(400 K)	96.2	98.7	3.99	47.8	1.29	1.06	1.67	1.83	69.8

Because of the orthorhombic crystal systems, the components of the elasticity tensor of the pure polymer matrix rest always nearly the one of a isotropic tensor whose the components obey to the following conditions:

$$C_{11} = C_{22} = C_{33}, \quad C_{12} = C_{13} = C_{23}, \quad C_{44} = C_{55} = C_{66} = \frac{1}{2}(C_{11} - C_{12}). \quad (4)$$

1
2
3
4
5
6
7
8
9
10
11
12
13
14
15
16
17
18
19
20
21
22
23
24
25
26
27
28
29
30
31
32
33
34
35
36
37
38
39
40
41
42
43
44
45
46
47
48
49
50
51
52
53
54
55
56
57
58
59
60
61
62
63
64
65

363 In contrast, all nanocomposite structures exhibit highly anisotropic behaviors. Indeed, the
364 elastic constants in XY-plane (C_{11} and C_{22}), which have similar values, are larger than the one
365 along the Z-axis (C_{33}). The nanocomposites' stiffness in XY-plane strongly depend on the in-
366 plane stiffness of clay platelets whereas its stiffness along the Z-axis strongly depends on the soft
367 polymeric phase. This result agrees well with previous numerical simulations of the mechanical
368 properties of clay cluster based on micromechanics methods, and the results obtained from these
369 atomistic MD simulations suggest that the anisotropic properties of PCN clusters should be taken
370 into account in continuum mechanics approaches to estimate the effective mechanical properties of
371 PCNs.

372 As can be seen from the Tab. 2, the elastic constants along the XY-plane decreases with
373 increasing number of cross-linked polymers in nanocomposite structures. This can be explained
374 by the fact that the elasticity *moduli* in the lateral directions are strongly affected by the stiffness
375 of clay layer due to the small volume of the organic phase in the intercalated structure. In this
376 case, the high values (around 125 GPa) have been derived. When the number of polymer increases,
377 the properties of the nanocomposites in lateral directions become more pronounced by the elastic
378 properties of polymer components, which show an approximative value of 60 GPa and 39 GPa for
379 the (N – 60E) and (N – 100E) systems, respectively. Interestingly, it is found that the the elastic
380 constant in the vertical direction of intercalated clay cluster (N – 20E) is smaller than that for
381 nearly exfoliated (N – 60E) or exfoliated structures (N – 100E). The small density of polymer
382 phase in the intercalated structure (N – 20E) discusses in the previous section, could contribute to
383 a bigger strain in the Z-axis, resulting to a smaller stiffness in comparison with two others systems
384 (N – 60E) and (N – 100E).

385 Moreover, one can observe that the elasticity constants of pure epoxy matrix and its nanocom-
386 posites decrease with increasing temperature. This statement reflects the typical behaviour of
387 thermoset polymer-based materials [55]. The stiffness of the pure epoxy matrix drastically de-
388 creases between 350 K and 400 K. However, much smaller change has been observed for the
389 nanocomposite cases.

390 The elastic properties of intercalated structure are less affected by the temperature than two
391 other nanocomposite structures, a result that is consistent with the behaviour of the glass transition
392 temperature previously discussed.

1
2
3
4
5
6
7
8
9
10
11
12
13
14
15
16
17
18
19
20
21
22
23
24
25
26
27
28
29
30
31
32
33
34
35
36
37
38
39
40
41
42
43
44
45
46
47
48
49
50
51
52
53
54
55
56
57
58
59
60
61
62
63
64
65

393 **4. Conclusion**

394 This work presents a novel molecular model approach to investigate the morphology and ther-
395 momechanical properties of epoxy/clay nanocomposites. The reactivity of the clay layer has been
396 taken into account using the reactive organomodifiant as aminosilanes, which are covalently grafted
397 to clay surface. The cross-linked epoxy molecules have been used as the polymer matrix. Different
398 molecular structures of PCNs, from intercalated to exfoliated one, have been generated based on
399 the amount of the polymer phase between the interlayer space. Molecular dynamics simulations
400 were conducted in order to determine structural arrangement of the constitutive components of
401 PCNs, the molecular interactions occurring in the interphase zone, and the influence of silicate layer
402 on the thermodynamic and elastic properties of these multi-functional materials. The interphase
403 thickness near the clay surface was identified as varying with the density of the organic phase. The
404 exfoliated structure showed a thicker interphase. The reactivity of the clay surface was quantified in
405 terms of RDFs between the reactive atoms, which are in the polymer phase and silane layer grafted
406 on the clay surface. The thermodynamic properties of the confined polymer in each structure were
407 also investigated in detail to identify the role of silicate layer on the properties of nanocomposites.
408 It has been showed that the polymer located close to clay surface strongly interacts with clay
409 surface and surfactant, hence enhancing its thermal stability. In addition, these molecular models
410 allowed us to estimate the effective elastic properties of the PCN models at different temperatures.
411 A high anisotropic behaviour of the PCNs at the nanoscale has been observed.

412 **Acknowledgment**

413 This work has benefited from a French government grant managed by ANR within the frame
414 of the national program of Investments for the Future ANR-11-LABX-022-01 (LabEx MMCD
415 project). Van Son Vo would like to thank Université Paris-Est and the Eduard-Zintl-Institut für
416 Anorganische and Physikalische Chemie and Research Cluster Center of Smart Interfaces (Technis-
417 che Universität Darmstadt, Darmstadt, Germany) for financial assistance in support of this work.
418 The authors would like to thank Michael C. Böhm and Florian Müller-Plathe from Technische
419 Universität Darmstadt for their comments on the draft of this article.

References

- [1] M. Alexandre and P. Dubois, "Polymer-layered silicate nanocomposites: preparation, properties and uses of a new class of materials," *Materials Science and Engineering: R: Reports*, vol. 28, no. 1, pp. 1–63, 2000.
- [2] S. Ray and M. Okamoto, "Polymer/layered silicate nanocomposites: a review from preparation to processing," *Progress in polymer science*, vol. 28, no. 11, pp. 1539–1641, 2003.
- [3] S. Pavlidou and C. Papispyrides, "A review on polymer-layered silicate nanocomposites," *Progress in polymer science*, vol. 33, no. 12, pp. 1119–1198, 2008.
- [4] B. Chen, J. Evans, H. Greenwell, P. Boulet, P. Coveney, A. Bowden, and A. Whiting, "A critical appraisal of polymer-clay nanocomposites," *Chemical Society Reviews*, vol. 37, no. 3, pp. 568–594, 2008.
- [5] Q. Zeng, A. Yu, and G. Lu, "Multiscale modeling and simulation of polymer nanocomposites," *Progress in Polymer Science*, vol. 33, no. 2, pp. 191–269, 2008.
- [6] N. Ghoniem, E. Busso, N. Kioussis, and H. Huang, "Multiscale modelling of nanomechanics and micromechanics: an overview," *Philosophical magazine*, vol. 83, no. 31-34, pp. 3475–3528, 2003.
- [7] F. Gardebien, A. Gaudel-Siri, J.-L. Brédas, and R. Lazzaroni, "Molecular dynamics simulations of intercalated poly (ϵ -caprolactone)-montmorillonite clay nanocomposites," *The Journal of Physical Chemistry B*, vol. 108, no. 30, pp. 10678–10686, 2004.
- [8] F. Gardebien, J. Brédas, and R. Lazzaroni, "Molecular dynamics simulations of nanocomposites based on poly (ϵ -caprolactone) grafted on montmorillonite clay," *The Journal of Physical Chemistry B*, vol. 109, no. 25, pp. 12287–12296, 2005.
- [9] J. Suter and P. Coveney, "Computer simulation study of the materials properties of intercalated and exfoliated poly (ethylene) glycol clay nanocomposites," *Soft Matter*, vol. 5, no. 11, pp. 2239–2251, 2009.
- [10] N. Sheng, M. Boyce, D. Parks, G. Rutledge, J. Abes, and R. Cohen, "Multiscale micromechanical modeling of polymer/clay nanocomposites and the effective clay particle," *Polymer*, vol. 45, no. 2, pp. 487–506, 2004.
- [11] L. Figiel and C. Buckley, "Elastic constants for an intercalated layered-silicate/polymer nanocomposite using the effective particle concept—a parametric study using numerical and analytical continuum approaches," *Computational Materials Science*, vol. 44, no. 4, pp. 1332–1343, 2009.
- [12] W. Xu, Q. Zeng, and A. Yu, "Young's modulus of effective clay clusters in polymer nanocomposites," *Polymer*, vol. 53, no. 17, pp. 3735–3740, 2012.
- [13] F. Piscitelli, P. Posocco, R. Toth, M. Fermiglia, S. Priol, G. Mensitieri, and M. Lavorgna, "Sodium montmorillonite silylation: unexpected effect of the aminosilane chain length," *Journal of Colloid and Interface Science*, vol. 351, no. 1, pp. 108–115, 2010.
- [14] Y. Chen, J. Chia, Z. Su, T. Tay, and V. Tan, "Mechanical characterization of interfaces in epoxy-clay nanocomposites by molecular simulations," *Polymer*, vol. 54, no. 2, pp. 766–773, 2013.
- [15] J. Ray, "Elastic constants and statistical ensembles in molecular dynamics," *Computer physics reports*, vol. 8, no. 3, pp. 109–151, 1988.
- [16] A. Silva, K. Dahmouche, and B. Soares, "Nanostructure and dynamic mechanical properties of silane-functionalized montmorillonite/epoxy nanocomposites," *Applied Clay Science*, vol. 54, no. 2, pp. 151–158, 2011.

1
2
3
4
5
6
7
8
9
10
11
12
13
14
15
16
17
18
19
20
21
22
23
24
25
26
27
28
29
30
31
32
33
34
35
36
37
38
39
40
41
42
43
44
45
46
47
48
49
50
51
52
53
54
55
56
57
58
59
60
61
62
63
64
65

[17] M. Huskić, M. Žigon, and M. Ivanković, “Comparison of the properties of clay polymer nanocomposites prepared by montmorillonite modified by silane and by quaternary ammonium salts,” *Applied Clay Science*, vol. 85, pp. 109–115, 2013.

[18] G. Sodeifian, H. R. Nikooamal, and A. A. Yousefi, “Molecular dynamics study of epoxy/clay nanocomposites: rheology and molecular confinement,” *Journal of Polymer Research*, vol. 19, no. 6, p. 9897, 2012.

[19] K. Anoukou, A. Zaoui, F. Zaïri, M. Nait-Abdelaziz, and J.-M. Gloaguen, “Molecular dynamics study of the polymer clay nanocomposites (pcns): Elastic constants and basal spacing predictions,” *Computational Materials Science*, vol. 77, pp. 417–423, 2013.

[20] G. Brindley and G. Brown, eds., *Crystal structures of clay minerals and their X-ray identification*. Oxford Univ. Press, 1980.

[21] Y. Choi, S. Lee, and S. Ryu, “Effect of silane functionalization of montmorillonite on epoxy/montmorillonite nanocomposite,” *Polymer Bulletin*, vol. 63, no. 1, pp. 47–55, 2009.

[22] V.-S. Vo, S. Mahouche-Chergui, J. Babinot, V.-H. Nguyen, S. Naili, and B. Carbonnier, “Photo-induced si-atrp for the synthesis of photoclickable intercalated clay nanofillers,” *RSC Advances*, vol. 6, no. 92, pp. 89322–89327, 2016.

[23] B. Kim, J. Choi, S. Yang, S. Yu, and M. Cho, “Influence of crosslink density on the interfacial characteristics of epoxy nanocomposites,” *Polymer*, vol. 60, pp. 186–197, 2015.

[24] C. Li, A. Browning, S. Christensen, and A. Strachan, “Atomistic simulations on multilayer graphene reinforced epoxy composites,” *Composites Part A: Applied Science and Manufacturing*, vol. 43, no. 8, pp. 1293–1300, 2012.

[25] S.-C. Shiu and J.-L. Tsai, “Characterizing thermal and mechanical properties of graphene/epoxy nanocomposites,” *Composites Part B: Engineering*, vol. 56, pp. 691–697, 2014.

[26] R. Rahman and A. Haque, “Molecular modeling of crosslinked grapheneepoxy nanocomposites for characterization of elastic constants and interfacial properties,” *Composites Part B: Engineering*, vol. 54, p. 353364, 2013.

[27] S. Yu, S. Yang, and M. Cho, “Multi-scale modeling of cross-linked epoxy nanocomposites,” *Polymer*, vol. 50, no. 3, pp. 945–952, 2009.

[28] T. Youngs, “Aten-an application for the creation, editing, and visualization of coordinates for glasses, liquids, crystals, and molecules,” *Journal of Computational Chemistry*, vol. 31, no. 3, pp. 639–648, 2010.

[29] R. Cygan, J.-J. Liang, and A. Kalinichev, “Molecular models of hydroxide, oxyhydroxide, and clay phases and the development of a general force field,” *The Journal of Physical Chemistry B*, vol. 108, no. 4, pp. 1255–1266, 2004.

[30] M. Frisch, G. Trucks, H. Schlegel, G. Scuseria, M. Robb, J. Cheeseman, G. Scalmani, V. Barone, B. Mennucci, G. Petersson, H. Nakatsuji, M. Caricato, X. Li, H. Hratchian, A. Izmaylov, J. Bloino, G. Zheng, J. Sonnenberg, M. Hada, M. Ehara, K. Toyota, R. Fukuda, J. Hasegawa, M. Ishida, T. Nakajima, Y. Honda, O. Kitao, H. Nakai, T. Vreven, J. J. Montgomery, J. Peralta, F. Ogliaro, M. Bearpark, J. Heyd, E. Brothers, K. Kudin, V. Staroverov, R. Kobayashi, J. Normand, K. Raghavachari, A. Rendell, J. Burant, S. Iyengar, J. Tomasi, M. Cossi, N. Rega, J. Millam, M. Klene, J. Knox, J. Cross, V. Bakken, C. Adamo, J. Jaramillo, R. Gomperts, R. Stratmann, O. Yazyev, A. Austin, R. Cammi, C. Pomelli, J. Ochterski, R. Martin, K. Morokuma, V. Zakrzewski, G. Voth,

- 1
2
3
4 495 P. Salvador, J. Dannenberg, S. Dapprich, A. Daniels, O. Farkas, J. Foresman, J. Ortiz, J. Cioslowski, and D. Fox,
5 496 "Gaussian 09 Revision D.01," 2009. Gaussian Inc. Wallingford CT 2009.
- 6 497 [31] H. Heinz, T.-J. Lin, R. Mishra, and F. Emami, "Thermodynamically consistent force fields for the assembly of
7 498 inorganic, organic, and biological nanostructures: The interface force field," *Langmuir*, vol. 29, no. 6, pp. 1754–
9 499 1765, 2013.
- 10 500 [32] C. Yong, "DL.FIELD-A force field and model development tool for DL.POLY," *CSE Frontiers*, vol. 2010,
11 501 pp. 38–40, 2010.
- 12 502 [33] M. Mazo, L. Manevitch, E. Gusarova, M. Shamaev, A. Berlin, N. Balabaev, and G. Rutledge, "Molecular
13 503 dynamics simulation of thermomechanical properties of montmorillonite crystal. 1. isolated clay nanoplate,"
14 504 *The Journal of Physical Chemistry B*, vol. 112, no. 10, pp. 2964–2969, 2008.
- 15 505 [34] X. Liu, X. Lu, R. Wang, H. Zhou, and S. Xu, "Interlayer structure and dynamics of alkylammonium-intercalated
16 506 smectites with and without water: A molecular dynamics study," *Clays and Clay Minerals*, vol. 55, no. 6,
17 507 pp. 554–564, 2007.
- 18 508 [35] B. Carrier, M. Vandamme, R. Pellenq, and H. Van Damme, "Elastic properties of swelling clay particles at finite
19 509 temperature upon hydration," *The Journal of Physical Chemistry C*, vol. 118, no. 17, pp. 8933–8943, 2014.
- 20 510 [36] H. Heinz, "Clay minerals for nanocomposites and biotechnology: surface modification, dynamics and responses
21 511 to stimuli," *Clay Minerals*, vol. 47, no. 2, pp. 205–230, 2012.
- 22 512 [37] H. Heinz, H. Koerner, K. Anderson, R. A. Vaia, and B. Farmer, "Force field for mica-type silicates and dynamics
23 513 of octadecylammonium chains grafted to montmorillonite," *Chemistry of Materials*, vol. 17, no. 23, pp. 5658–
24 514 5669, 2005.
- 25 515 [38] G. Zartman, H. Liu, B. Akdim, and H. Pachter, R. and Heinz, "Nanoscale tensile, shear, and failure properties
26 516 of layered silicates as a function of cation density and stress," *The Journal of Physical Chemistry C*, vol. 114,
27 517 no. 4, pp. 1763–1772, 2010.
- 28 518 [39] I. Todorov, W. Smith, K. Trachenko, and M. Dove, "DL.POLY_3: new dimensions in molecular dynamics
29 519 simulations via massive parallelism," *Journal of Materials Chemistry*, vol. 16, no. 20, pp. 1911–1918, 2006.
- 30 520 [40] U. Essmann, L. Perera, M. Berkowitz, T. Darden, H. Lee, and L. Pedersen, "A smooth particle mesh ewald
31 521 method," *The Journal of chemical physics*, vol. 103, no. 19, pp. 8577–8593, 1995.
- 32 522 [41] C. Li and A. Strachan, "Molecular scale simulations on thermoset polymers: A review," *Journal of Polymer
33 523 Science Part B: Polymer Physics*, vol. 53, no. 2, pp. 103–122, 2015.
- 34 524 [42] M. Parrinello and A. Rahman, "Crystal structure and pair potentials: A molecular-dynamics study," *Physical
35 525 Review Letters*, vol. 45, no. 14, p. 1196, 1980.
- 36 526 [43] K. Van Workum and J. de Pablo, "Improved simulation method for the calculation of the elastic constants of
37 527 crystalline and amorphous systems using strain fluctuations," *Physical Review E*, vol. 67, no. 1, p. 011505, 2003.
- 38 528 [44] J. Tack and D. Ford, "Thermodynamic and mechanical properties of epoxy resin dgebf crosslinked with detda
39 529 by molecular dynamics," *Journal of Molecular Graphics and Modelling*, vol. 26, no. 8, pp. 1269–1275, 2008.
- 40 530 [45] H. Fan and M. Yuen, "Material properties of the cross-linked epoxy resin compound predicted by molecular
41 531 dynamics simulation," *Polymer*, vol. 48, no. 7, pp. 2174–2178, 2007.
- 42 532 [46] F. Garcia, B. Soares, V. Pita, R. Sánchez, and J. Rieumont, "Mechanical properties of epoxy networks based
43 533

- 1
2
3
4 533 on dgeba and aliphatic amines,” *Journal of Applied Polymer Science*, vol. 106, no. 3, pp. 2047–2055, 2007.
- 5 534 [47] E. Brown, S. R. White, and N. Sottos, “Fatigue crack propagation in microcapsule-toughened epoxy,” *Journal*
6 535 *of Materials Science*, vol. 41, no. 19, pp. 6266–6273, 2006.
- 7
8 536 [48] C. Li and A. Strachan, “Molecular dynamics predictions of thermal and mechanical properties of thermoset
9 537 polymer epon862/detda,” *Polymer*, vol. 52, no. 13, pp. 2920–2928, 2011.
- 10 538 [49] Q. Yang, X. Li, L. Shi, X. Yang, and G. Sui, “The thermal characteristics of epoxy resin: Design and predict
11 539 by using molecular simulation method,” *Polymer*, vol. 54, no. 23, pp. 6447–6454, 2013.
- 12
13 540 [50] C. Hadden, B. Jensen, A. Bandyopadhyay, G. Odegard, A. Koo, and R. Liang, “Molecular modeling of epon-
14 541 862/graphite composites: interfacial characteristics for multiple crosslink densities,” *Composites Science and*
15 542 *Technology*, vol. 76, pp. 92–99, 2013.
- 16
17 543 [51] G. Odegard, T. Clancy, and T. Gates, “Modeling of the mechanical properties of nanoparticle/polymer com-
18 544 posites,” *Polymer*, vol. 46, no. 2, pp. 553–562, 2005.
- 19
20 545 [52] C. Li and A. Strachan, “Molecular simulations of crosslinking process of thermosetting polymers,” *Polymer*,
21 546 vol. 51, no. 25, pp. 6058–6070, 2010.
- 22
23 547 [53] A. Shokuhfar and B. Arab, “The effect of cross linking density on the mechanical properties and structure of the
24 548 epoxy polymers: molecular dynamics simulation,” *Journal of Molecular Modeling*, vol. 19, no. 9, pp. 3719–3731,
25 549 2013.
- 26
27 550 [54] S. Yang and J. Qu, “Computing thermomechanical properties of crosslinked epoxy by molecular dynamic sim-
28 551 ulations,” *Polymer*, vol. 53, no. 21, pp. 4806–4817, 2012.
- 29
30 552 [55] J. Choi, S. Yu, S. Yang, and M. Cho, “The glass transition and thermoelastic behavior of epoxy-based nanocom-
31 553 posites: A molecular dynamics study,” *Polymer*, vol. 52, no. 22, pp. 5197–5203, 2011.
- 32
33 554 [56] N. Nouri and S. Ziaei-Rad, “A molecular dynamics investigation on mechanical properties of cross-linked polymer
34 555 networks,” *Macromolecules*, vol. 44, no. 13, pp. 5481–5489, 2011.
- 35
36 556 [57] V. Varshney, S. Patnaik, A. Roy, and B. Farmer, “A molecular dynamics study of epoxy-based networks:
37 557 cross-linking procedure and prediction of molecular and material properties,” *Macromolecules*, vol. 41, no. 18,
38 558 pp. 6837–6842, 2008.
- 39
40
41
42
43
44
45
46
47
48
49
50
51
52
53
54
55
56
57
58
59
60
61
62
63
64
65